Respiratory Flow-Sound Relationship and Estimation by Parametric and Nonparametric Methods using Features of Tracheal Sound

by
Marziyeh Golabbakhsh

A Thesis submitted to the Faculty of Graduate Studies of University of Manitoba in partial fulfillment of the requirements for the degree of

MASTER OF SCIENCE

Department of Electrical and Computer Engineering
University of Manitoba
Winnipeg, Manitoba, Canada

THE UNIVERSITY OF MANITOBA

FACULTY OF GRADUATE STUDIES

*****

COPYRIGHT PERMISSION

"Respiratory Flow-Sound Relationship and Estimation by Parametric and Nonparametric Methods using Features of Tracheal Sound"

BY

Marziyeh Golabbakhsh

A Thesis/Practicum submitted to the Faculty of Graduate Studies of The University of Manitoba in partial fulfillment of the requirement of the degree

Of

MASTER OF SCIENCE

ABSTRACT

In this study several features of tracheal sound were studied in order to estimate flow from tracheal sound. These features included the average power of tracheal sound (P_{ave}), the envelope of the fifth level coefficient of the wavelet transform of the tracheal sound signal (E_{a5}) and f_{max}, f_{mean} and f_{peak} of tracheal sound spectrum. The relationship between flow and these features were studied considering a few models for each feature. Then, the better model representing the relationship between flow and a particular feature was selected for flow estimation. Parametric methods in addition to nonparametric methods including adaptive filters and Neural Networks were used for flow estimation.

The least error for flow estimation with parametric methods, which was 9 ± 3 % and 10 ± 4 % for inspiration and expiration respectively, was obtained using exponential model describing P_{ave} and flow relationship. Considering nonparametric methods, the estimation error was the least for the third order adaptive filter which was 10 ± 3 % and 11 ± 4 % for inspiration and expiration respectively. The input of this filter was again the average power of the tracheal sound. Therefore, in a sense, these two techniques were similar in their model.

The effect of aging on model parameters for f_{max} and P_{ave} was investigated considering second-degree polynomial model for f_{max} and exponential model for P_{ave}. The results showed a considerable shift of f_{max} toward lower frequencies with age. However, there was not a conclusive result for describing the relationship between age and P_{ave}.

ACKNOWLEDGMENTS

I would like to express my deep thanks and appreciation to my supervisor Dr Zahra Moussavi for her continuous support and encouragement during my master program.

Thanks to my dear colleague Mohammad Aboofazeli who was always happy to help me and answer my questions.

I would also like to thank my kind professors: Dr. Miroslaw Pawlak, Dr. Joe LoVetri, Dr. Steve Onyshko and Dr. Gabriel Thomas.

I am grateful to all graduate students in Biomedical Engineering Lab, Mahsa Taleb Pourazad, Lisa Lazareck, Aimee Betker, Irina Hossain, and January Gnitecki for sharing their knowledge and experience with me.

Finally I thank my husband Keyvan for his patience and support during my graduate studies.

TABLE OF CONTENTS

LIST OF FIGURES

LIST OF TABLES

CHAPTER 1

INTRODUCTION

1.1 MOTIVATION

Relationship between respiratory sound and flow has always been of great interest for physicians and researchers due to its diagnostic applications. One of the important investigation areas of respiratory sounds concerns the relationship between respiratory sounds and flow. Respiratory sounds are measured by either accelerometers or microphones. Respiratory flow is normally measured either by direct means (using pneumotachograph or nasal cannulae connected to pressure transducer (Figure 1.1)) or by indirect means (detecting chest and/or abdominal movements), which is often called respiratory effort. Figure 1.2 shows a detailed summary of these methods [Tarrant *et al.*, 1997].

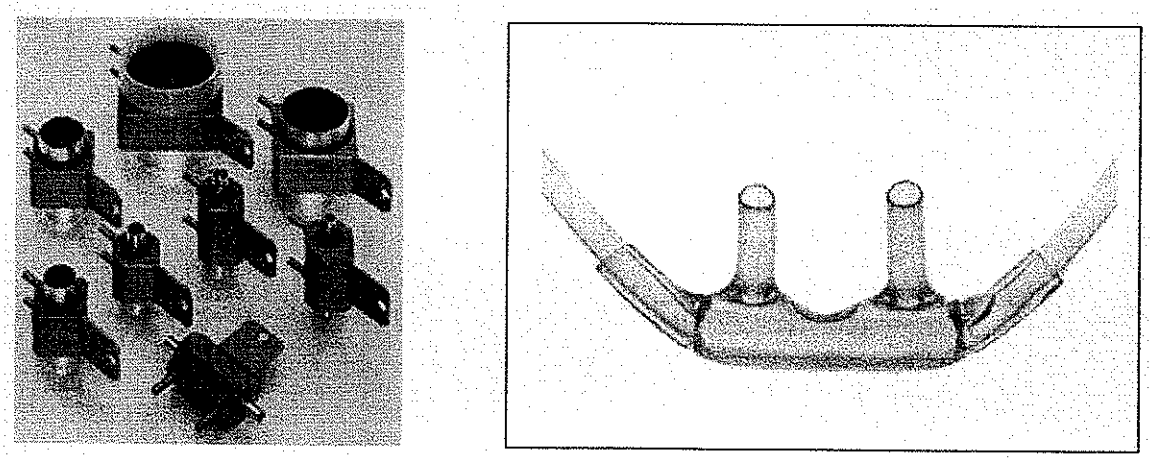

Figure 1.1. Spirometry devices: pneumotachograph (left) and nasal cannulae (right)

Some of these methods are used together to lessen the inaccuracy of the measurement. A combination of nasal cannulae connected to a pressure transducer along with chest and/or

abdominal respiratory movement detection is known as the best method for flow measurement in swallowing and respiration studies [Tarrant *et al.*, 1997].

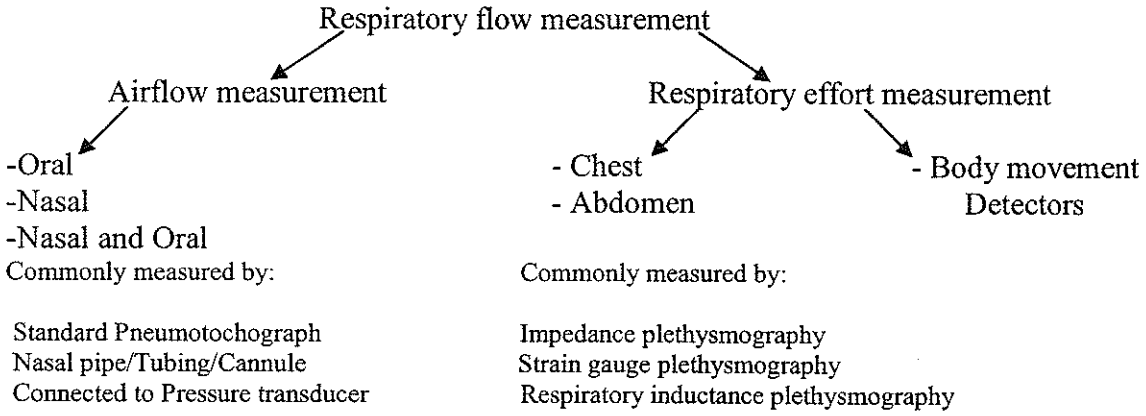

Figure 1.2. A summary of methods for flow measurement.

Many of flow measurement methods, although adequate for respiration monitoring in apnea studies, are less useful in swallowing and feeding assessments [Tarrant *et al.*, 1997]. Also, application of these techniques to young children or patients with neurological impairments is a challenge, as they usually do not cooperate during signal recording. The situation is worse when working with patients with physical deformities and poor postural control [Moussavi *et al.*, 2000]. There have been attempts to replace the cumbersome flow measurement techniques by estimating it through tracheal sounds [Moussavi *et al.*, 2000; Yap & Moussavi, 2002; Que *et al.*, 2002]. The goal of this thesis was to continue that line of research and investigate flow-sound relationship thoroughly in order to develop a robust method for flow estimation from tracheal respiratory sound.

1.2 BACKGROUND

The primary function of the respiratory system is to supply the blood with oxygen in order for the blood to deliver oxygen to all parts of the body. The respiratory system does this through breathing. When we breathe, we inhale oxygen and exhale carbon dioxide. This exchange of gases is the respiratory system's means of getting oxygen to the blood. Respiration is achieved through the mouth, nose, trachea, lungs, and diaphragm. Oxygen enters the respiratory system through the mouth and the nose. It then passes through the larynx and trachea, which enters the chest cavity. In the chest cavity, the trachea splits into two smaller tubes called the bronchi. Each bronchus then divides again forming the bronchial tubes. The bronchial tubes lead directly into the lungs where they divide into many smaller tubes, which connect to tiny sacs called alveoli. The anatomy of respiratory system is shown in Figure 1.3.

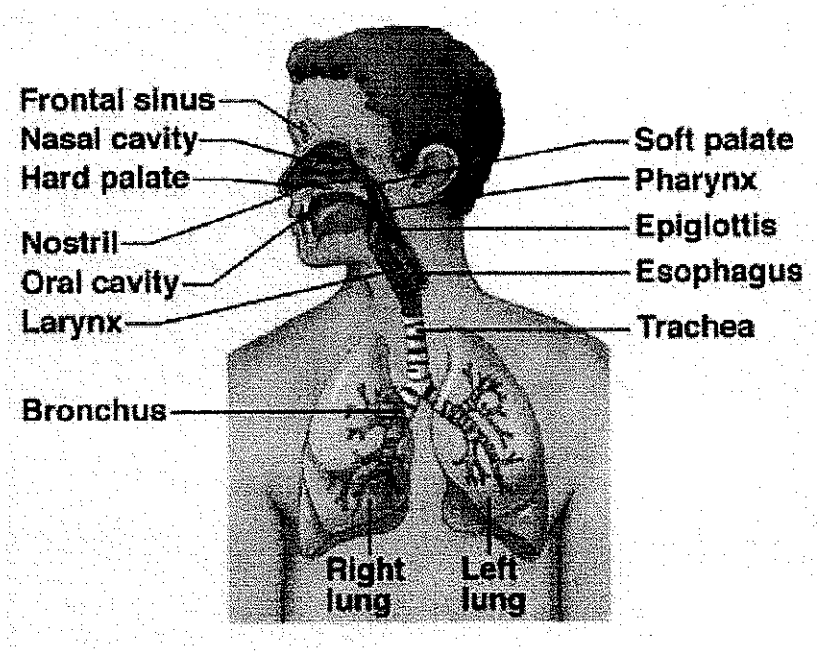

Figure 1.3. Anatomy of the respiratory system.

The breathing sounds recorded on the neck at the suprasternal notch over the extrathoracic trachea, are called tracheal sounds. Tracheal sound signal is relatively large in amplitude; and its spectrum covers a frequency range from less than 100 Hz to more than 1500 Hz, with a sharp attenuation in energy above cutoff frequency of approximately 800 Hz [Gavriely *et al.*, 1981]. Tracheal sound has clearly separate phases and is directly related to respiratory flow [Gavriely *et al.*, 1996]. The placement of sensors over the trachea is relatively easy with least interference from body hair, garments, etc.

Tracheal sound is mainly generated by turbulent of flow in upper airways, including pharynx, glottis, and subglottic regions. Sound pressure waves within the airway gas and airway wall motion cause the vibrations that reach the neck surface, where tracheal sounds are recorded. Because there are various sound sources in the upper airways and the sensor at the neck is relatively in short distance and there is no interposition of lung tissue, tracheal sounds are often known as a more pure and less filtered breath sound [Pasterkamp *et al.*, 1997].

Since the invention of *Laënnec's* stethoscope in 1817, physicians use this instrument as a routine tool to listen to respiratory sounds for clinical diagnosis. However, auscultation with a stethoscope has many limitations. Diagnosis with stethoscope is a subjective perception by individual physician. Also stethoscopes do not provide a frequency-independent transmission of sounds. Rather, they amplify frequencies below 112 Hz and attenuate higher frequencies [Abella *et al.*, 1992].

Respiratory sound analysis has seen a major innovation in recent years, as modern technology and digital signal processing techniques present immense advantages for

capturing, storage, analysis and communication of respiratory sounds. Over the last decades, researches have found relationships between respiratory sounds and diseases such as asthma, obstructive sleep apnea, respiratory infections, swelling, malformations and tumors [Bohadana *et al.*, 1994; Avital *et al.*, 1988; Hida *et al.*, 1988; Pasterkamp *et al.*, 1996; Rietveld & Rijssenbeek-Nouwens, 1998; Sanna *et al.*, 1991; Yonemaru *et al.*, 1993]. Also many researchers have studied the relationship of tracheal sound and flow to airway geometry and anatomical properties of respiratory tract [Brancatisano *et al.*, 1983; Sanchez & Pasterkamp, 1993; Harper *et al.*, 2003]. Some effort has been done to computationally model the anatomy of the respiratory tract to investigate its acoustical behavior and to know more about sound transmission and reflection measurements [Van Den Berg, 1960; Ishizaka *et al.*, 1976; Fredberg, 1978; Nemerovskii, 1980; Jackson *et al.*, 1989; Hudde & Slatky, 1989; Wodicka *et al.*, 1989; Harper *et al.*, 2001, 2003]. Tracheal sound measurement provides valuable and in many cases unique information about respiratory health and disease. Apnea (usually defined to be a cessation of breathing of 10 seconds or more) monitoring by simple acoustical detection of tracheal sounds is an application that has been successfully applied [Krumpe & Cummiskey, 1980; East, 1985; Sanna *et al.*, 1991; Beckerman *et al.*, 1982]. Narrowing below the glottis can also be investigated by analysis of tracheal sound [Pasterkamp *et al.*, 1997; Hida *et al.*, 1988]. In some studies tracheal sound has been used for classifying healthy individuals from patients with pulmonary disease [Mussel *et al.*, 1990; Jeon *et al.*, 1999]. For instance, it was found that the frequency of peak amplitude and mean frequency of the breath sound spectra of patients were higher than those of healthy subjects [Mussel *et al.*, 1990]. Monitoring of tracheal respiratory sounds has been recognized as a way of diagnosing

nocturnal respiratory dysrhythmias [Sanna *et al.*, 1991]. Diagnosis of spontaneous cough in asthma from the results of continuous tracheal sound recording is another application of repiratory sound analysis [Rietveld & Rijssenbeek-Nouwens, 1998]. In another study tracheal sounds of patients with tracheal stenosis (a narrowing of the trachea) and that of normal persons were investigated. It was found that the peak sound amplitude at approximately 1 kHz and the sound power in a bandwidth from 600 to 1300 Hz were higher for patients [Yonemaru *et al.*, 1993].

Overall, respiratory sound analysis is of interest for its diagnostic applications as mentioned above. On the other hand, respiratory flow measurement is an essential part of these studies. However, as described in previous section, flow measurement is a challenge especially when it is applied to young children or patients with neurological impairments. Furthermore, it cannot be accurately measured during swallowing or feeding assessment.

As mentioned before relationship between tracheal sound and flow has long been recognized [Forgacs, 1978] and attempts have been made to replace the cumbersome flow measurement by flow estimation from tracheal sounds [Soufflet *et al.*, 1990; Moussavi *et al.*, 2000; Yap & Moussavi, 2002; Que *et al.*, 2002]. Despite the magnitude of the investigation in this field, the results are still not robust enough to replace flow measurement by estimating it from tracheal sounds. This study was an attempt to investigate several models for tracheal sound-flow relationship in order to find a robust method for flow estimation by acoustical means.

The main objectives of this study were:

- to investigate several features and models describing tracheal sound-flow relationship for a wide range of flow (0-3 L/s).
- to evaluate the capability of the model to estimate flow from tracheal sound.
- to investigate the capability of nonparametric methods to estimate flow from tracheal sound.

1.3 OUTLINE OF THE THESIS

Chapter 1 - This chapter presents the motivation and background information for this thesis. It briefly presents different applications of respiratory sound analysis including an overview of respiratory system and tracheal sounds' characteristics and the objectives of this thesis.

Chapter 2 - This chapter gives a brief review of past researches done on tracheal sound analysis and its relationship with respiratory flow.

Chapter 3 - This chapter describes the data acquisition and instrumentation used in this research, the signal processing techniques to find the features of tracheal sound which have a consistent relationship with flow and different methods to estimate flow from those features.

Chapter 4 - The results of investigating relationship between different features of tracheal sound and flow are summarized in this chapter. It includes results of flow estimation with parametric as well as nonparametric techniques.

Chapter 5 - This chapter provides discussions on the results, as well as conclusions.

Chapter 6 - This chapter discusses a few directions for possible future works.

CHAPTER 2

LITERATURE REVIEW

The relationship between respiratory flow and breath sounds has been under investigation for several years by different researchers. However, the main interest has been primarily on either deriving features related to the frequency spectrum of the breath sound signal, or classifying patients from healthy individuals rather than using breath sound for flow estimation.

Early investigation on the relationship between tracheal sound and flow revealed that increasing the flow caused parallel upward shift of the spectral curve, while the general pattern of the tracheal sound spectrum remained unchanged [Leblanc *et. al.*, 1970; Charbonneau *et. al.*, 1987]. Other studies showed that increasing flow modified both intensity and the frequency distribution of the tracheal sound spectrum [Ploysongsang *et al.*, 1982; Lessard & Wong, 1986; Kraman *et al.*, 1998; Charbonneau *et al.*, 1987; Forgacs *et al.*, 1978; Soufflet *et al.*, 1990; Mussell *et al.*, 1990, 1992; Gavriely *et al.*, 1996; Moussavi *et al.*, 2000; Yap & Moussavi, 2002; Harper *et al.*, 2003].

Some of the investigators have used mathematical functions to quantify the relationship between features of tracheal sound and flow [Shykoff *et al.*, 1988; Lessard & Wong, 1986; Gavriely *et al.*, 1996; Yap & Moussavi, 2002; Que *et al.*, 2002]. Most of these studies have focused on flow rates greater than 0.5 L/s because it is more difficult to derive a consistent pattern for very low flow. Furthermore, there exists a range of flow (minimum critical flow) where no relationship between breath sound amplitude and flow can be obtained [Shykoff *et al.*, 1988; Gavriely *et al.*, 1996; Yap & Moussavi, 2002]. Therefore, the relationship between the sound amplitude and flow can be obtained only

when the sound amplitude exceeds the background noise. This minimum critical flow has been found to be about 0.2 and 0.4 L/s for tracheal and lung sounds, respectively [Chi-Lem *et al.*, 1997]

About two decades ago, the relationship between tracheal sounds and flow was discussed by measuring flow-induced noise (jet noise) in a model of the trachea with an artificial glottis and concluded a third order relationship between the two variables [Olson *et al.*, 1984, 1985].

Using statistical analysis, a quadratic relationship between the breath sound and flow was demonstrated [Shykoff *et al.*, 1988]. However, they found that the envelope of the recorded tracheal sounds had consistent fluctuation that limited their accuracy for flow estimation and therefore they did not estimate flow.

Power relationship between tracheal sound amplitude (*BSA*) and flow was reported [Gavriely *et al.*, 1996], as described by the following equation:

$$BSA = kF^{\alpha}, \qquad 2.1$$

where F is flow in L/s and α and k are some constants. By amplitude, they meant the average power of tracheal sound, which was calculated over the frequency band of 100-2400 Hz. They did no attempt to estimate flow employing this model.

In another study [Harper *et al.*, 2003] the effects of flow on tracheal sound was investigated after building a dynamic model of respiratory tract. Tracheal sounds were measured from four healthy subjects at target flow rates of 0.5, 1, 1.5 and 2 L/s and also during nontargeted breathing. Both the simulated and measured spectra illustrated that sound power were increasing with increasing flow, with smaller incremental changes at

higher flow rates. They also calculated average power of tracheal sound over the frequency band of 300-600 Hz and reported that the spectral power trended to increase with flow for all four subjects. They did not derive a model for this relationship and therefore, did not attempt to estimate flow.

Frequency-based features of tracheal sound have been also studied by many researchers. In a study the relationship between flow and frequency spectrum of tracheal sounds was investigated [Lessard & Wong, 1986 & 1988]. Tracheal sounds were measured at six constant flow rates (0.25, 0.5, 0.75, 1, 1.25 and 1.5 L/s) with an electric stethoscope placed at the anterior cervical triangle. The three parameters from the spectrum of tracheal sound were calculated. Those parameters were the mean frequency, the frequency of the maximum power, and the highest frequency at which the power decreased to 10% of the maximum power. The general linear model multivariate analysis of variance (ANOVA) was used to test the hypotheses that the characterizing parameters of the respiratory sounds are constant for all flow rates within the sample population. The results showed a direct linear relationship between the spectrum parameters and flow in the range from 0.25 L/s to about 0.75 L/s but it leveled off as the flow rate increased beyond 0.75 L/s during inspiration or expiration.

In another study, using flow rates of 1.6, 2.1 and 2.6 L/s, it was claimed that the spectral parameters of the tracheal sound were flow independent. However, the tracheal sounds were significantly modified by the flow transducer in that study [Mussell *et al.*, 1992], making the results questionable.

On the other hand, there is a comparison study of some different flow estimation models from tracheal sounds for the flow rates up to 1.5 L/s [Soufflet *et al.*, 1990]. Each

subject performed recording tests for three different flow rates (shallow, normal, high). In order to estimate instantaneous flow from tracheal sounds eight methods divided in two groups of four were investigated. In the first group (reference curves method), it was assumed that a relationship existed between sound and flow and thus reflected by the variations of some parameters. Four different parameters were tested: mean amplitude of the sound, mean amplitude of the spectrum, mean frequency of the spectrum and the product of the mean amplitude and mean frequency. During the calibration phase, for each parameter a reference curve was built, representing the variations of each parameter versus flow being specific to each subject. Then, the flow was estimated by calculating the parameter and using the reference curve corresponding to that flow. In the second group, they made a hierarchical clustering analysis of sound spectra and tested two kinds of spectra (direct and normalized) as well as two ways of associating flow to a given cluster that led to four other methods. In one case only one reference flow was associated to a cluster and in the other cases, there were six reference flows associated to a class, making distinction whether the flow belonged to inspiration or expiration and considering three recordings of each subject separately. The comparison of the various methods showed that no method was superior to the others. However, the hierarchical clustering analysis gave finer flow estimation than the reference curve method; an improvement being achieved by a significant increase in calculation time as mentioned in the study. For all methods, the mean error in estimation of the flow rate was reported to be 14%, except one method, which had an error of 31%. The methods were also computationally costly [Soufflet *et al.*, 1990].

More recently flow was estimated from breath sound intensity during quiet

breathing and therefore, almost exclusively on constant flow about 0.5 L/s [Que *et al.*, 2002]. Flow and tracheal sounds were measured simultaneously during two separate 30-s intervals. From the first 30-s period the relationship between flow and sound was determined. This relationship was then used to calibrate the model and derive flow and volume from the amplitude of the sound signal of the next 30 s period. They assumed a linear relationship model between flow and tracheal breath sound amplitude and used least squares linear regression to find the model parameters. A threshold sound value above which the relationship between sound amplitude and flow could be determined was thus defined for each subject and the model was calculated for flows greater than the threshold, and the flow below the threshold was estimated by linear interpolation. Because they were more interested in volume than in flow, they used the error in volume estimation as the criterion of their method's accuracy. The error in estimating tidal volume was less than 15% in all subjects. This study was not robust because it considered only tidal flow and also it used a relatively long period of flow and its corresponding tracheal sound (50%) for calibration.

Average power of tracheal and lung sounds has already been used to detect respiratory phases and breath onsets independent of flow [Moussavi *et al.*, 2000]. 100% accuracy in respiratory phase detection was achieved without using the measured flow signal. The outcomes of that study were used for flow estimation in another study, in which several possible relationships between flow and average power of tracheal sound (P_{ave}) were studied over different frequency bands [Yap & Moussavi, 2002]. Three relationships, linear ($P_{ave}=kF$), power ($P_{ave}=kF^{\alpha}$) and exponential ($P_{ave}=ke^{F\alpha}$) between flow and P_{ave}, were investigated. In all subjects breath sounds were recorded at low (0-

0.4 L/s), medium (0.4-0.8 L/s) and high (0.8-1.4 L/s) flow rates. It was found that the exponential relationship described the relationship better than the other two relationships and hence, it was employed to estimate flow. The model was chosen as:

$$F_{est} = c_1 log(P_{ave}) + c_2, \qquad 2.2$$

where F_{est} is the estimated flow and c_1 and c_2 are the model coefficients. When the coefficients of the model in Eq. 2.2 were derived from a certain flow rate considered as the base and then used to estimate other flow rates, the estimation was consistently underestimated or overestimated. In order to remedy this problem, they modified the model by applying a scaling factor to justify for different target flows. They defined a scaling factor in the form of a ratio between the average power of the segment that its associated flow is being estimated and the average power of the base segments, which were used to derive the coefficients. Therefore, they modified Eq. 2.2 as:

$$F_{est} = (c_1 log(P_{ave}) + c_2)(\frac{P_{segment}}{P_{base}})^k, \qquad 2.3$$

where k is a constant that is determined from a few known breath sounds with flow that were assumed to be available for calibration. For example, if the model coefficients c_1 and c_2 were derived from medium target flow, k consisting of k_{low} and k_{high} was determined by minimizing the error using two known breaths at low and high flow rates, respectively [Yap & Moussavi, 2002].

In that study P_{ave} was calculated from nine different frequency bands and it was found that over the range of 150-450 Hz, P_{ave} had the highest correlation with flow. Also they showed that the least estimation error was achieved using upper 40% of flow, when changing the lower limit of flow from 10% to 90%. The overall error was found to be

6.7± 1.79 % and 2.98±0.78 % for inspiration and expiration, respectively. In that method, the model coefficients are derived from three breaths at one target flow (medium), but the model still needs further calibration for scaling factor, which is achieved by assuming that there are some copies of breath at other target flow rates available for calibration. Therefore, it still requires the subjects to breathe at different flow rates. Also, it is not mentioned in their work how the tracheal sound is grouped to one of the three different regions during estimation.

All of the discussed methods in this section have used only parametric techniques for modeling the relationship between flow and tracheal sound. Also, the flow rate was either constant [Que *et al.*, 2002] or variable but at most up to 1.5 L/s [Soufflet *et al.*, 1990; Yap & Moussavi. 2002].

In this study, flow estimation from tracheal sounds was investigated for a wide range of flow up to 3 L/s considering different parametric models -some common to those previously investigated- as well as nonparametric methods.

CHAPTER 3

METHODS

3.1 DATA

Data from 15 subjects were studied in this research. Subjects were from two groups: 5 healthy adults (1 male) aged 31.8 ± 8.1 years (Group I), 10 healthy children (6 males) aged 9.6 ± 2.9 years (Group II). Data of Group I was collected at the Respiratory Acoustics Laboratory, University of Manitoba. Informed consent was obtained from subjects or their parents (guardian) before recording. The study was approved by the Human Research Ethics Board of University of Manitoba, Faculty of Medicine, Ethics Committee. Data of Group II were adopted from a previous study [Yap & Moussavi, 2002] which used the same data acquisition system. Physical characteristics of subjects participated in this study are given in Table 3.1.

Data recordings were performed with the subject seated in a soundproof chamber (no. 101549, Industrial Acoustics Company, Bronx, NY). The tracheal and lung sounds were recorded by Siemens accelerometers (EMT25C) placed over suprasternal notch and chest wall. In this study, however, only tracheal sounds were used. With a nose clip in place, flow was measured by a mouthpiece attached to a calibrated pneumotachograph (Fleich No3). To reduce the friction of the sensors' cables against the subject's skin or clothing which causes noise artifacts that could be detected by the accelerometer, the cables were held away from the subject with tape loops. Subjects were instructed to breathe at four different flow rates -low (0-7.5 ml/s/Kg), tidal (7.5-15 ml/s/Kg), medium (15-22.5 ml/s/Kg) and high (22.5-50 ml/s/Kg)- with five breaths at each target flow followed by a 10 s breath hold to obtain a reference for background noise. A visual

display of flow signal helped the subjects to keep their target breathing as instructed. After each recording the tracheal sounds were played-back and the spectrograms of the recorded signals were examined to see if there were any noise artifacts in the recorded signal.

Table 3.1. Physical characteristics of subjects.

Subject No.	Gender	Age (yr)	Weight (kg)
Healthy Adults (Group I)			
1	F	26	53
2	F	26	64
3	F	26	64
4	M	38	90
5	F	43	54.5
Healthy Children (Group II)			
1	M	4	20
2	M	9	61
3	F	13	36
4	M	13	50
5	M	11	42
6	M	7	32
7	F	11	36
8	F	11	44
9	M	7	30
10	F	10	34

The breath sound signals were amplified, band-pass filtered (50-2500 Hz). The filtered signals were then digitized at a 10240 Hz sampling rate using a 12-bit analog-to-digital converter on a National Instruments PC-mounted card (PCI-1200, National Instruments, Austin, TX). Flow signal was digitized simultaneously with breath sounds at the same sampling rate but it was later decimated to 320 Hz.

3.2 SIGNAL PROCESSING

Inspiratory and expiratory tracheal sounds were analyzed separately, because (i) the resistance at the vocal cord changes with respiratory phase; and (ii) mechanisms to provide each respiratory phase sound are different [Mussel *et al.*, 1990].

The estimation error was defined as:

$$\text{Error} = \left| \frac{mean(F_{est}) - mean(F_{actual})}{mean(F_{actual})} \right| \qquad 3.1$$

where the mean( ) was calculated from the average of the upper 15% of the flow signal, F_{est} is the estimated flow and F_{actual} is the actual flow. For different methods of flow estimation, the estimation error was calculated for each subject and then averaged between the subjects.

3.2.1 Average Power of Tracheal Sound

The tracheal sound signals were sequestered into 1024-sample segments (100 ms), with 50% overlap between successive segments. The power spectrum density (PSD) of each segment was calculated using FFT and applying a Hanning window to each segment. Average spectral power (P_{ave}) was calculated over the frequency band 150-450 Hz because previous studies found this frequency band as the best for flow estimation from tracheal sound [Yap & Moussavi, 2002]. Figure 3.1 illustrates an example of the calculated P_{ave} of a recorded tracheal sound signal along with its spectrogram and the corresponding flow signal.

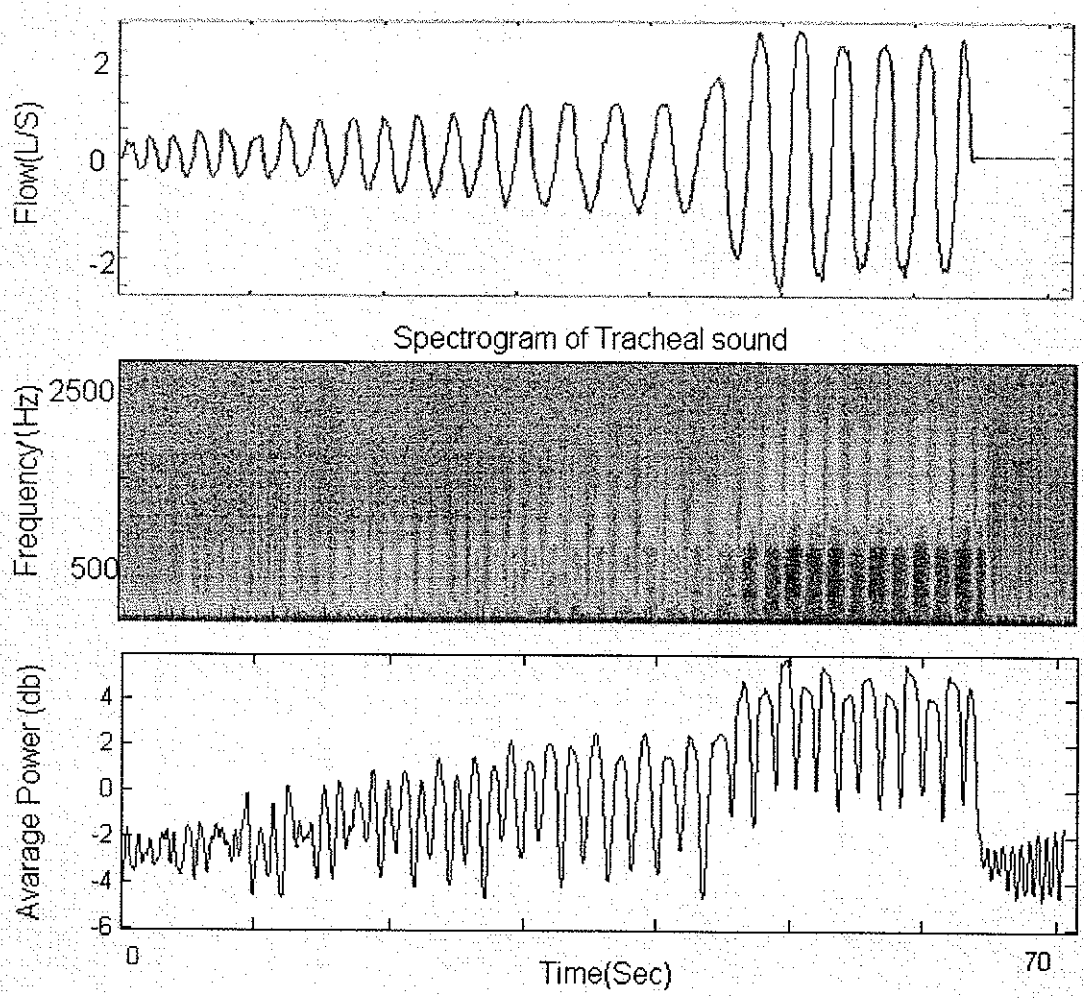

Figure 3.1. The spectrogram of a typical tracheal sound signal (middle graph) and P_{ave} calculated over 150-450 Hz frequency band (bottom graph) with its corresponding flow signal (top graph).

3.2.2 Frequency- Based Features of Tracheal Sound

The following parameters were calculated from the PSD of the tracheal sound signal at each target flow: maximum frequency (f_{max}), mean power frequency (f_{mean}) and frequency of the highest power (f_{peak}). f_{max} was defined as the frequency at which the PSD of inspiration/expiration reached the PSD of the breath hold segments. f_{mean} was defined as:

$$f_{mean} = \frac{\int f.S(f)df}{\int S(f)df}, \qquad 3.2$$

where $S(f)$ is the amplitude of the PSD of the signal at frequency f. f_{peak} was defined as the frequency at which PSD reached its first maximum after the frequency of 100 Hz. Figure 3.2 shows an example of the frequency features of the PSD of a typical signal.

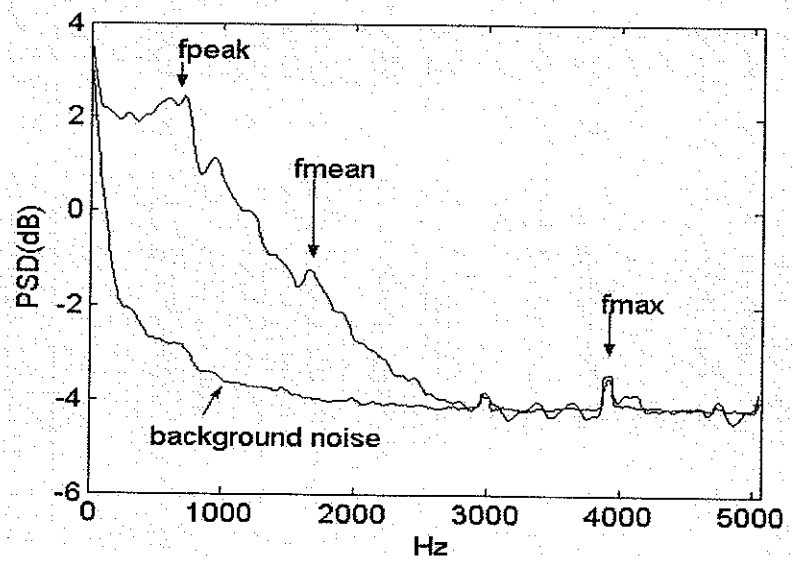

Figure 3.2. A typical PSD of a breath segment and the frequency features.

3.2.3 Wavelet Transform of Tracheal Sound

Wavelet analysis consists of decomposing a signal or an image into a hierarchical set of approximations and details. A wavelet is a waveform of limited duration that has an average value of zero and a defined function $\psi(t)$ [Bratteli *et al.*, 2002]. By dilation, or changes of scale(s), and translations, i.e., time domain window regions of size τ, families of wavelets are formed based on the main or "mother" wavelet, $\psi(t)$,

$$\psi_{s,\tau}(t) = \frac{1}{\sqrt{s}}\psi\left(\frac{t-\tau}{s}\right), \qquad s > 0, \tau \in \Re \qquad 3.3$$

where s is the dilation parameter and τ is the translation parameter [Mallat, 1989].

The continuous wavelet transform (CWT) is defined as the integral of the time-domain signal multiplied by scaled and shifted versions of the wavelet function $\psi(t)$:

$$a_{s,\tau} = \int_{-\infty}^{\infty} f(t)\psi_{s,\tau}(t)dt, \qquad 3.4$$

The results of the CWT are many wavelet coefficients a_i, which are functions of the scale and position. Wavelet analysis allows the use of long time intervals where more precise low-frequency information is required, and shorter regions for high-frequency information (Figure 3.3).

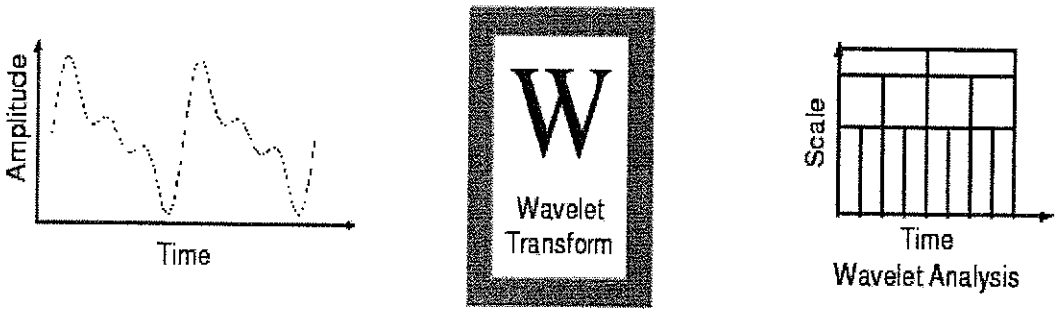

Figure 3.3. Wavelet Transform

Some examples of the mother wavelet functions commonly used in signal processing are shown in Figure 3.4. The names of the Daubechies family wavelets are written dbN, where N is the order.

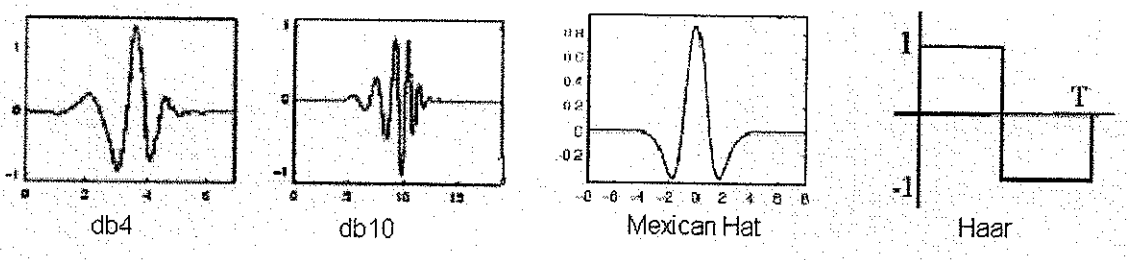

Figure 3.4. Examples of some commonly used mother wavelet functions.

In this study the one-dimensional CWT of the tracheal sound was calculated using db4 mother wavelet with 12 scales. Comparing different wavelet coefficients with flow, it was found that the fifth coefficient of the wavelet transform had the highest correlation with flow. Hence, the envelope of the fifth coefficient (Ea_5) of the CWT was obtained using Hilbert transform. Hilbert Transform of a real valued signal *x(t)* is defined as

$$y(t) = H_x(t) = \frac{1}{\pi} \int_{-\infty}^{\infty} \frac{x(\tau)}{\tau - t} d\tau, \qquad 3.5$$

where the integral is taken in the principal value sense. That is, the integral is defined as the limit of integrals taken over bounded intervals with regions around x deleted. Specifically we have

$$H_x(t) = \lim_{\varepsilon \to 0, R \to \infty} \frac{1}{\pi} \left(\int_{-R}^{x-\varepsilon} \frac{x(\tau)}{\tau - t} d\tau + \int_{x+\varepsilon}^{R} \frac{x(\tau)}{\tau - t} d\tau \right). \qquad 3.6$$

When a real signal *x(t)* and its Hilbert Transform $y(t) = H_x(t)$ are used to form a new complex signal $z(t) = x(t) + jy(t)$, the signal *z(t)* is the "analytic signal" corresponding to the real signal *x(t)* with all "negative frequencies" of *x(t)* being filtered out [Oppenheim & Schafer, 1998]. The analytic signal is useful in calculating instantaneous attributes of a time series, especially the amplitude and frequency. The instantaneous amplitude is the amplitude of the complex Hilbert transformed signal *z(t)*, and the instantaneous frequency is the time rate of change of the instantaneous phase angle. Due to its simplicity, Hilbert Transform is a very popular method for envelope detection of time varying signals. It was observed that the Hilbert Transform of the fifth coefficient, E_{a5}, followed flow signal quite well (Figure 3.5) and hence, the relationship between these two signals were investigated further.

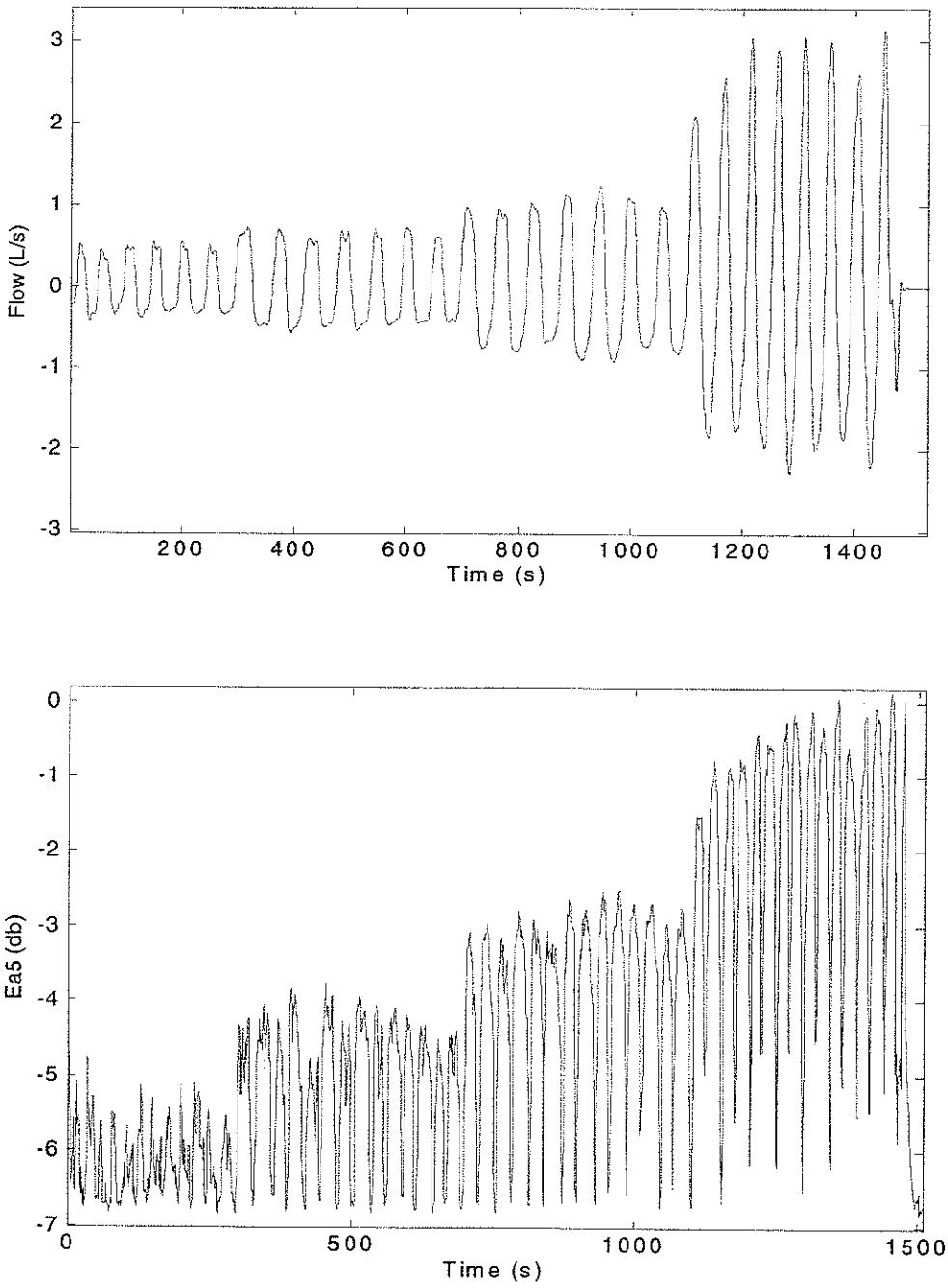

Figure 3.5. Envelope of the fifth coefficient of wavelet transform of a typical tracheal sound (bottom graph) along with its corresponding flow (top graph).

3.3 PILOT STUDIES

3.3.1 Relationship between P_{ave} and Flow

Since the main interest was to estimate the target flow accurately and flow usually reaches a plateau in its upper 15% (Figure 3.6), this region was used for investigating different models describing relationship between flow and P_{ave}.

The following models were studied to find a better model describing the relationship between flow and P_{ave}. The first two models were adopted from a previous study [Yap & Moussavi, 2002].

1) Exponential Model: $F = c_1 \log(P_{ave}) + c_2$ 3.7

2) Power Model: $\log(F) = c_1 \log(P_{ave}) + c_2$ 3.8

3) 2nd degree Polynomial Model: $F = c_1 P_{ave}^{\ 2} + c_2 P_{ave} + c_3$ 3.9

4) 3rd degree Polynomial Model: $F = c_1 P_{ave}^{\ 3} + c_2 P_{ave}^{\ 2} + c_3 P_{ave} + c_4$ 3.10

where F is the mean of upper 15% of target flow and c_1, c_2 and c_3 are some constants. To compare different models, Mean Square Error (MSE) between the actual values of flow and the fitted curves was calculated for the four different models and averaged between all the subjects. MSE of different models and correlation coefficient of exponential and power models, are shown in Tables 3.2 and 3.3.

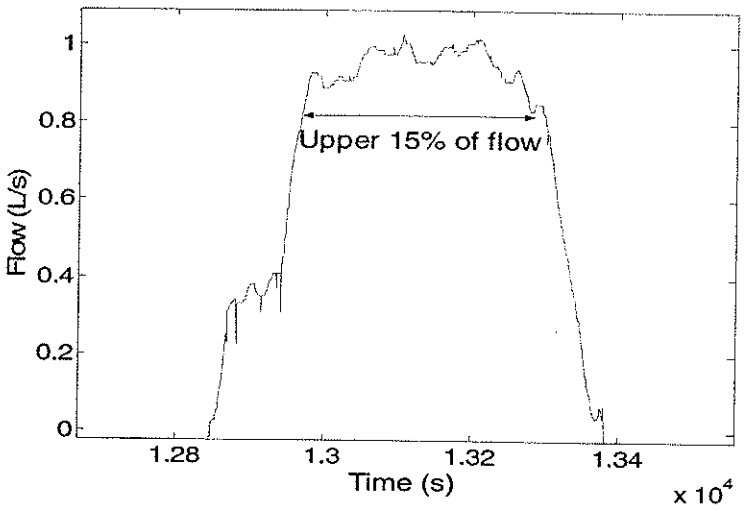

Figure 3.6. A typical example of one inspiration showing its upper 15%.

It was shown that if the coefficients of the model in Equations 3.7 to 3.10 were derived from a certain flow rate and then used to estimate other flow rates, the estimated flow was constantly underestimated or overestimated [Yap & Moussavi, 2002]. For this reason, we could not choose a better model based on MSE only. Data should be preprocessd to determine which model is better in terms of estimation. Therefore, data of five subjects from Group I, who breathed at four distinct target flow rates, were selected. For each subject the time-domain data of three different target flows were used to find the model coefficients and then the left-out flow rate was estimated with that model. The estimation error was calculated using Equation 3.1 and averaged between the subjects for different models. Table 3.4 displays the estimation error for different models during inspiration. Based on the results of Tables 3.2 to 3.4, the exponential model (Eq. 3.7) was chosen as a better model for describing the relationship between flow and $P_{ave.}$ Figure 3.7 shows the relationship between P_{ave} and flow for one of the subjects.

Table 3.2. MSE of different models describing flow and P_{ave} relationship.

MSE ($\mu \pm \sigma$)	Inspiration	Expiration
Exponential model	0.05 ± 0.05	0.07 ± 0.05
Power model	0.18 ± 0.38	0.07 ± 0.13
2nd degree polynomial model	0.05 ± 0.06	0.05 ± 0.05
3rd degree polynomial model	0.03 ± 0.04	0.03 ± 0.02

Table 3.3. Correlation coefficient of exponential and power models describing flow and P_{ave} relationship.

Correlation Coefficient ($\mu \pm \sigma$)	Inspiration	Expiration
Exponential model	0.9 ± 0.05	0.86 ± 0.07
Power model	0.87 ± 0.07	0.92 ± 0.06

Table 3.4. Estimation error for different models when estimating flow from P_{ave}.

Model	Estimation of high flow rate	Estimation of medium flow rate	Estimation of tidal flow rate	Estimation of low flow rate
Exponential model	0.14 ± 0.11	0.25 ± 0.15	1.5 ± 0.4	7.24 ± 7.3
Power model	0.63 ± 0.52	0.09 ± 0.02	1.1 ± 0.2	7.7 ± 6.8
2nd degree polynomial model	35.8 ± 56.33	2.67 ± 4.92	2.5 ± 0.5	8.87 ± 6.51
3rd degree polynomial model	96 ± 14	0.16 ± 0.09	1.2 ± 0.6	8.08 ± 6.04

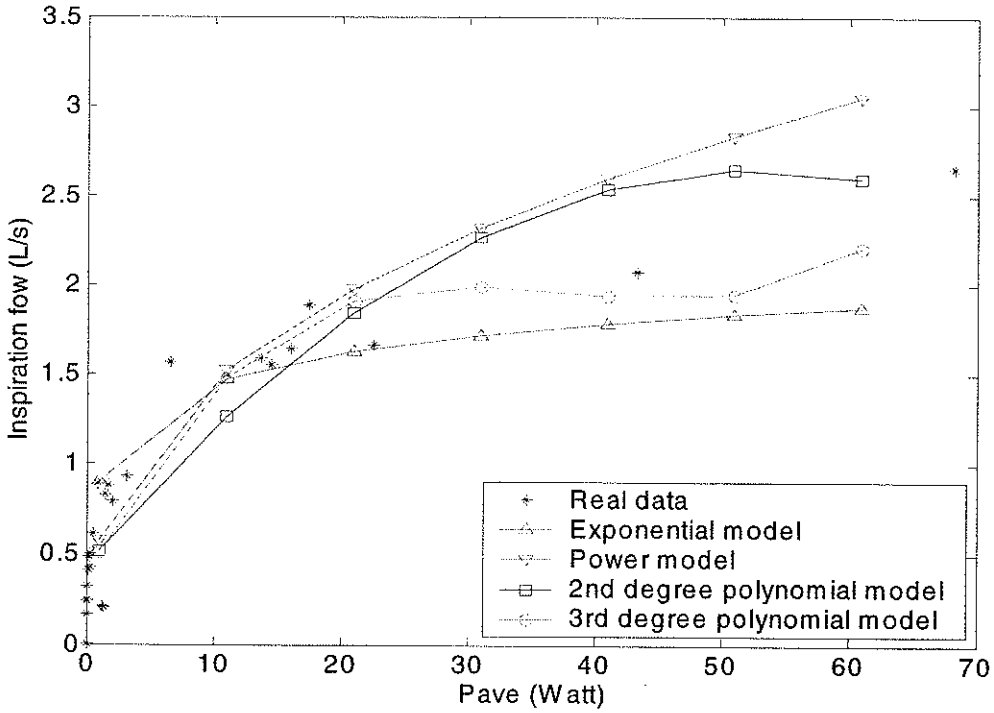

Figure 3.7. Relationship between P_{ave} and flow using different models fitted to data.

3.3.2 Relationship between Frequency-Based Features of Tracheal Sound and Flow

Three models were investigated to describe the relationship between flow and frequency- based features of tracheal sound.

$$1)\ F = c_1 f^2 + c_2 f + c_3, \qquad 3.11$$

$$2)\ F = c_1 \exp(f) + c_2, \qquad 3.12$$

$$3)\ F = c_1 log(f) + c_2, \qquad 3.13$$

where F is the mean of upper 15% of target flow, f is the frequency-based feature and c_1, c_2 and c_3 are constants. For f_{max} models 3.11 and 3.12 were employed, while for f_{mean}

and f_{peak}, model 3.11 and model 3.13 were used. For each model, the MSE between the actual data and the fitted curve was calculated and averaged between the subjects.

Tables 3.5 and 3.6 show the values of MSE for different frequency-based features and models for inspiration and expiration, respectively. Table 3.7 displays the correlation coefficients of the model in Eq. 3.12 and Eq. 3.13. Figure 3.8 demonstrates the relationship between flow and frequency-based features for one of the subjects.

Table 3.5. MSE ($\mu \pm \sigma$) of different models between frequency-based features and flow during inspiration.

(a)

Model	f_{peak}	f_{mean}
$F = c_1 \log(f) + c_2$	0.3 ± 0.26	0.21 ± 0.21
$F = c_1 f^2 + c_2 f + c_3$	0.27 ± 0.26	0.17 ± 0.19

(b)

Model	f_{max}
$F = c_1 exp(f) + c_2$	0.06 ± 0.05
$F = c_1 f^2 + c_2 f + c_3$	0.05 ± 0.04

Table 3.6. MSE ($\mu \pm \sigma$) of different models between different frequency-based features and flow during expiration.

(a)

Model	f_{peak}	f_{mean}
$F = c_1 \log(f) + c_2$	0.23 ± 0.22	0.20 ± 0.16
$F = c_1 f^2 + c_2 f + c_3$	0.16 ± 0.19	0.18 ± 0.15

(b)

Model	f_{max}
$F = c_1 exp(f) + c_2$	0.1 ± 0.07
$F = c_1 f^2 + c_2 f + c_3$	0.06 ± 0.04

Table 3.7. Correlation coefficient of the exponential model (Eq. 3. 12 & Eq. 3.13) between different frequency-based features and flow.

(a)

Exponential Model: $F = c_1 \log(f) + c_2$	f_{peak}	f_{mean}
Inspiration	0.33 ± 0.17	0.46 ± 0.28
Expiration	0.29 ± 0.15	0.40 ± 0.13

(b)

Exponential Model: $F = c_1 exp(f) + c_2$	f_{max}
Inspiration	0.83 ± 0.13
Expiration	0.77 ± 0.26

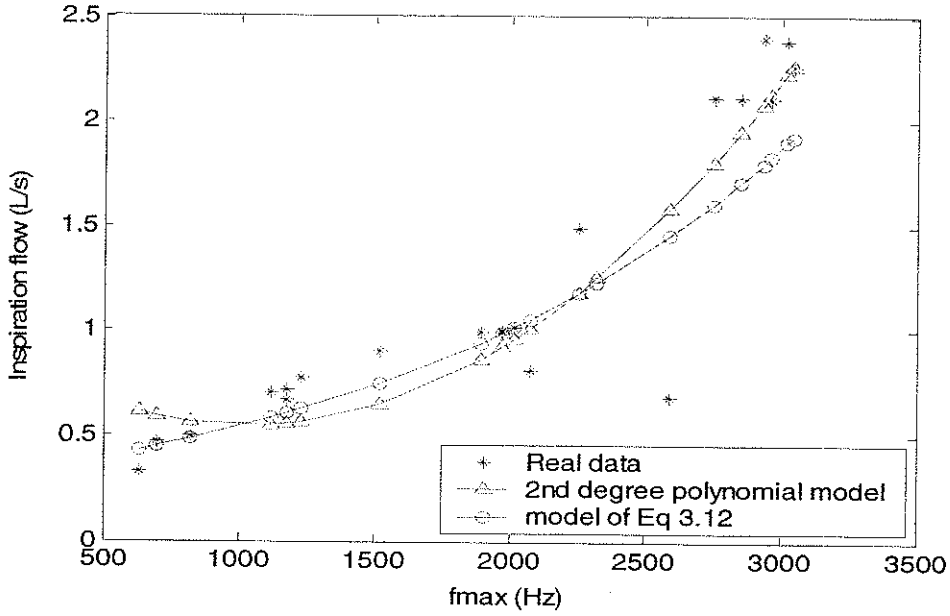
Inspiration flow (L/s)
fmax (Hz)
Real data
2nd degree polynomial model
model of Eq 3.12

(a)

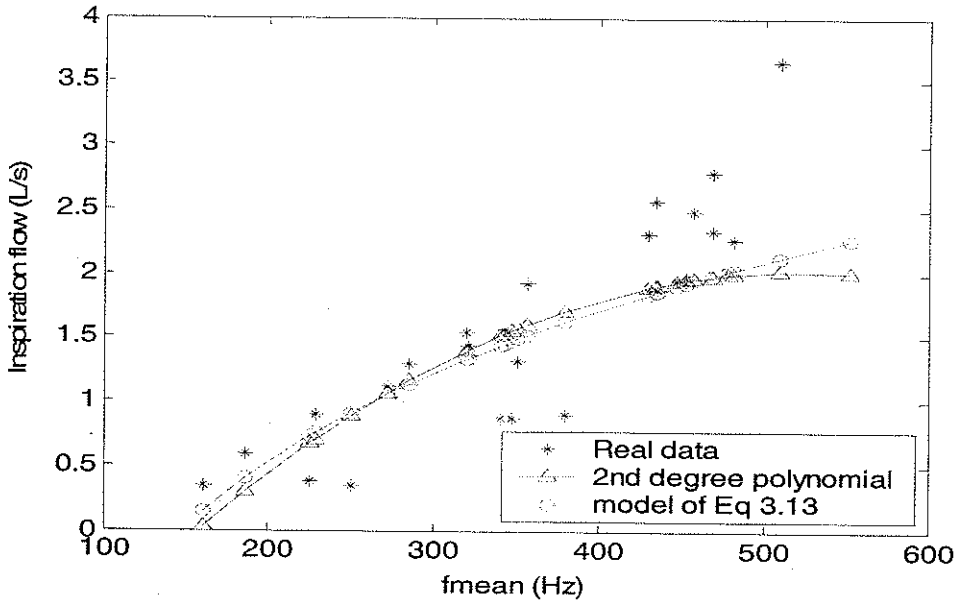
Inspiration flow (L/s)
fmean (Hz)
Real data
2nd degree polynomial
model of Eq 3.13

(b)

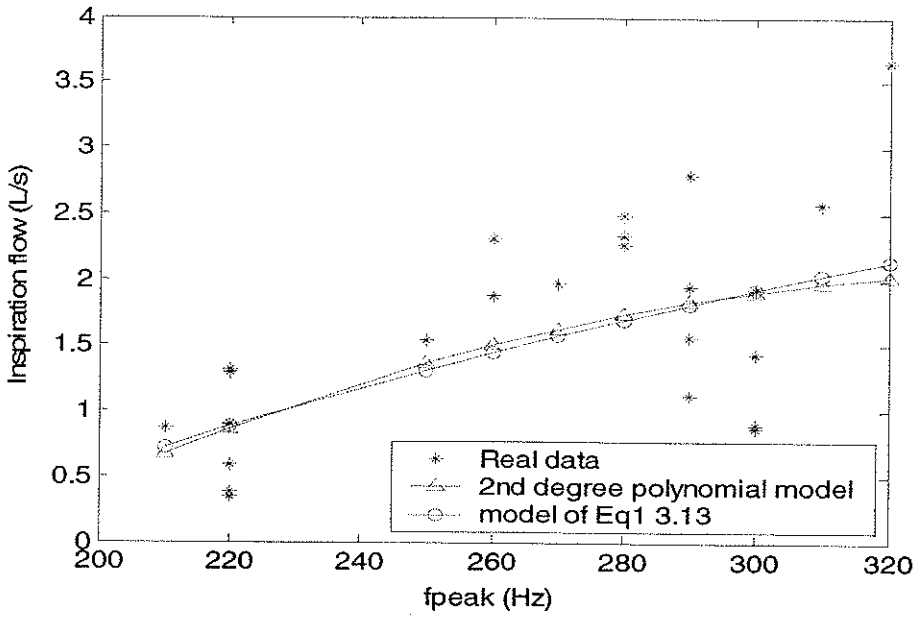

(c)

Figure 3.8. Relationship between frequency-based features and flow using different models fitted to data.

While there was not a strong relationship between f_{peak} and flow and f_{mean} and flow, f_{max} showed a considerable relationship with flow. Furthermore, the 2nd degree polynomial model showed slightly better fit than the exponential models using f_{max}. The results were consistent for both inspiration and expiration.

Because the correlation coefficient of the exponential model of Eq. 3.12 was low comparing to that of the exponential model that describing flow and P_{ave} (Eq. 3.7), we did not consider Eq. 3.12 for flow estimation.

Considering the 2nd degree polynomial relationship, f_{max} had lowest MSE among the models using frequency-based features. Therefore the 2nd degree polynomial model of this group (Eq. 3.11) was employed for flow estimation.

3.3.3 Relationship between E_{a5} and Flow

To investigate the relationship between E_{a5} and flow, the following two models were studied.

$$1) \text{ Power Model: } \log(F) = c_1 \log(E_{a5}) + c_2, \tag{3.14}$$

$$2) \text{ Linear Model: } F = c_1 E_{a5} + c_2, \tag{3.15}$$

where F is the flow signal.

The MSE between actual values of flow and the fitted curves and correlation coefficients used for relationship between flow and E_{a5} are shown in Tables 3.8 and 3.9, respectively. Figure 3.9 is an example of the relationship between flow and E_{a5} and the fitted models for one of the subjects.

Table 3.8. MSE ($\mu \pm \sigma$) of different models describing flow and E_{a5} relationship.

Model	Inspiration	Expiration
Power model	0.02 ± 0.02	0.03 ± 0.02
Linear model	0.04 ± 0.04	0.02 ± 0.02

Table 3.9. Correlation coefficients ($\mu \pm \sigma$) of different models describing flow and E_{a5} relationship.

Model	Inspiration	Expiration
Power model	0.92 ± 0.07	0.91 ± 0.07
Linear model	0.86 ± 0.09	0.87 ± 0.09

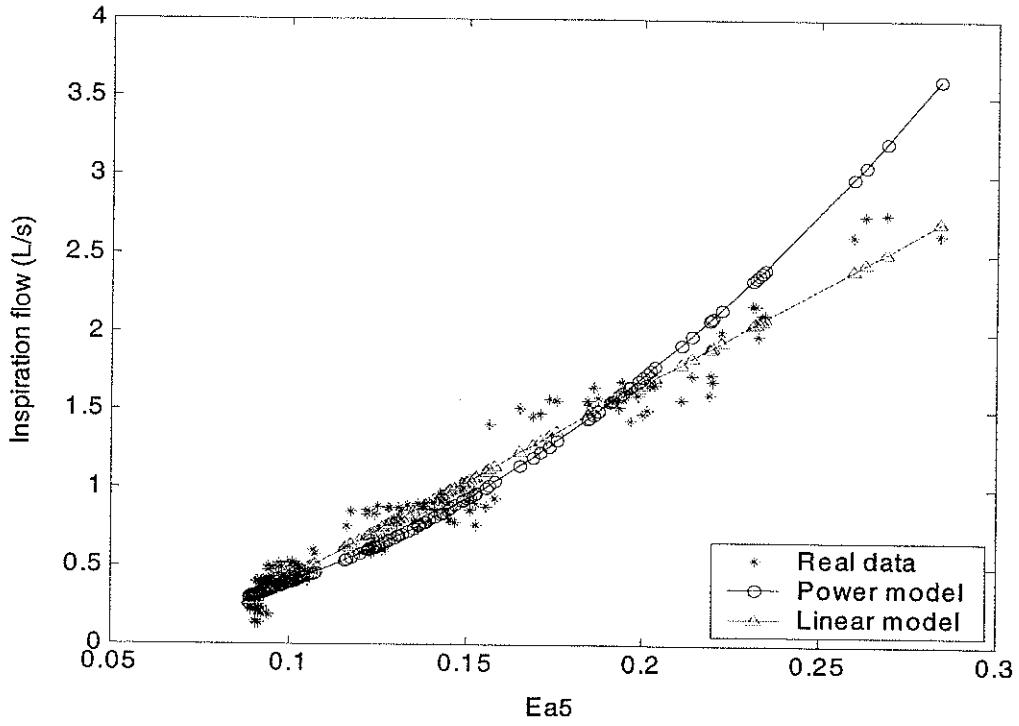

Figure 3.9. Relationship between Ea5 and flow using different models fitted to data.

The data was preprocessed to evaluate estimation error for different models in the same manner used for the models using P_{ave}. Table 3.10 displays the estimation error for different models during inspiration. As it can be seen the models' performance were not very different in regard to the estimation error. Therefore, the power relationship model, which had the least MSE and highest correlation coefficient, was chosen as the better

model for describing the relationship between flow and the E_{a5} and was later used for estimating flow. The model coefficients, for each region, were derived by fitting a line to the data of one breath of that region which was assumed to be available during calibration. Figure 3.10 shows that there is a linear relationship between flow (dB) and E_{a5} (dB).

Table 3.10. Estimation error for different models when estimating flow from Ea5.

Model	Estimation of high flow rate	Estimation of medium flow rate	Estimation of tidal flow rate	Estimation of low flow rate
Power model	0.19 ± 0.08	0.15 ± 0.06	0.45 ± 0.23	1.20 ± 0.77
Linear model	0.17 ± 0.10	0.13 ± 0.06	0.35 ± 0.30	1.17 ± 0.73

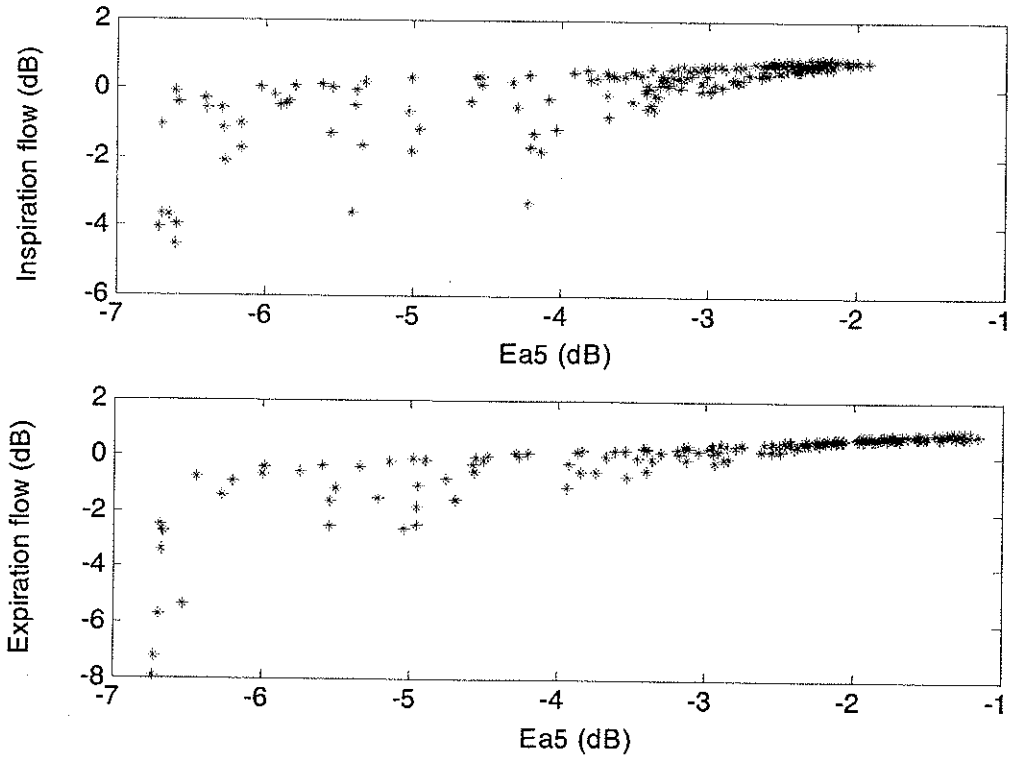

Figure 3.10. Flow (dB) versus E_{a5} (dB) during inspiration and expiration.

3.4 FLOW ESTIMATION BY PARAMETRIC METHODS

Based on the results of the pilot studies, the models, which had either higher correlation coefficient or less MSE, were chosen for flow estimation. These chosen models were exponential model using P_{ave}, power model using E_{a5} and 2nd degree polynomial model using f_{max}.

For exponential model between P_{ave} and flow, upper 40% of flow was used because previous studies have shown that the correlation coefficient is the highest in this region [Yap & Moussavi, 2002]. For the other two models, target flow optimization was done considering different upper X% (X=15, 25, 40, 65 & 90) of flow for deriving the models' coefficients. The values of MSE and correlation coefficient (for power and exponential models) between actual values of flow and the fitted curves were compared to determine an optimum flow region for deriving the models' coefficients. However, the results were not conclusive for a flow region to be superior to others. Hence, the upper 40% of flow was used for flow estimation with the three different models for the sake of consistency.

In order to derive the model's coefficients, given the vast variety of the flow-sound relationship between the subjects, all flow estimation methods are in need of calibration. It was assumed that flow signal of at least one breath from each target flow is available for calibration. In this study flow was estimated using two types of calibration:

- Type 1: The model was calibrated for all flow rates at the same time, i.e., only one set of coefficients was used for every target flow rate.
- Type 2: The model was calibrated for every flow rate separately, i.e., three or four sets of coefficients were used for each target flow.

In order to divide tracheal sound signal to different target flow regions without using the flow signal, E_{a5} signal was used instead of the P_{ave} of tracheal sound signal because E_{a5} showed a better correspondence with target flow rate (Figure 3.5) compared to P_{ave} ; In Fig 3.1 it was not very different between low and tidal flow rates. Therefore, for each subject tracheal sound signal was divided to different target flow regions based on E_{a5} signal by defining a threshold for each region.

3.5 FLOW ESTIMATION BY NONPARAMETRIC METHODS

3.5.1 Adaptive Filters

The ability of an adaptive filter to operate satisfactorily in an unknown environment and track time variations of input statistics makes the adaptive filtering a powerful technique for signal processing. Indeed, adaptive filters have been successfully applied in diverse fields such as prediction, plant identification, denoising signals, etc. Although these applications are different in nature, they have a basic structure in common: the output of the filter tries to follow the input by minimizing the energy of error between the output and a desired response. The adjustable filter coefficients may take the form of tap weights, reflection coefficients, or rotation parameters depending on the filter structure employed. However, the essential difference between the various applications of adaptive filtering arises in the manner in which the desired response is extracted [Haykin, 2002].

The class of adaptive filtering used in this study was identification configuration. In the class of applications dealing with identification, the adaptive filter is used to provide a linear model that represents the best fit (in some sense) to an unknown plant. The plant and the adaptive filter are driven by the same input. The plant output supplies the desired

response for the adaptive filter. The schematic of the identification configuration is shown in Figure 3.11.

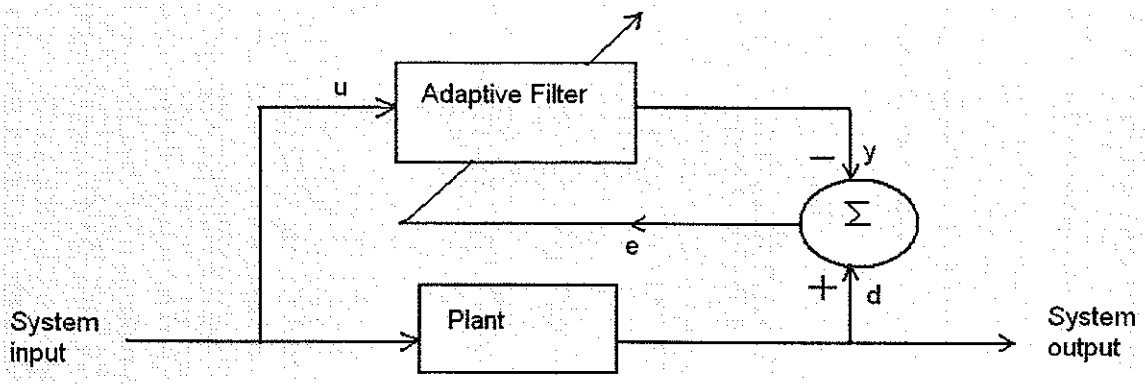

Figure 3.11. Identification Configuration.

Least Mean Square (LMS) Algorithm

The LMS algorithm or Widrow-Hoff learning algorithm is a linear adaptive filtering algorithm, which in general consists of two basic processes:

1. A *filtering process*, which involves computing the output of a linear filter in response to an input signal and generating an estimation error by comparing this output with a desired response.
2. An *adaptive process*, which involves the automatic adjustment of the parameters of the filter in accordance with the estimation error.

In this study, P_{ave} of the tracheal sound signal was used as the input of the filter and flow as the desired response. Therefore, the output of the filter was considered as the estimated flow, which is a linear combination of the P_{ave}. This can be formulated as the following:

$$\hat{flow}(n) = \sum_{k=0}^{M-1} w_k P_{ave}(n-k) = \hat{w}^H(n) \cdot u(n) \quad , \qquad 3.16$$

where M is the order of the filter, $\hat{w}(n) = [\hat{w}_0(n), \hat{w}_1(n), ..., \hat{w}_{M-1}(n)]^T$ is the weight vector at time index n, H indicates the Hermitian transpose, $u(n) = [P_{ave}(n), P_{ave}(n-1), ..., P_{ave}(n-M+1)]^T$ is the input signal and $\hat{flow}$ is the estimated flow as the output signal. The estimation error, e, at time index n is calculated as

$$e(n) = flow(n) - \hat{flow}(n). \tag{3.17}$$

During the adaptive process, the filter is optimized with minimizing the cost function, $J(n)$, defined as

$$J(n) = E[|e(n)|^2] \tag{3.18}$$

by taking the gradient vector

$$\nabla J(n) = -2\gamma_{ud} + 2\Gamma_{uu}\hat{w}(n) \ , \tag{3.19}$$

where $\gamma_{ud} = E[u(n)flow(n)]$ is the cross correlation between the input and the desired output, and $\Gamma_{uu} = E[u(n)u^H(n)]$ is the autocorrelation matrix of the input vector. Using the estimates $\hat{\Gamma}_{uu}(n) = u(n)u^H(n)$ and $\hat{\gamma}_{ud}(n) = u(n)flow(n)$, the steepest descent algorithm is then employed to obtain the following formula for adapting the tap weight vector

$$\hat{w}(n+1) = \hat{w}(n) + \mu u(n)[flow(n) - u^H(n)\hat{w}(n)] = \hat{w}(n) + \mu u(n)e^*(n) \ , \tag{3.20}$$

where μ is the adaptation step size, subject to the following constraint

$$0 < \mu < \frac{2}{MS_{\max}}, \tag{3.21}$$

where $S_{\max}$ is the maximum value of the power spectral density of the tap inputs $u(n)$ and M is the number of tap weights [Haykin, 2002].

Typically one epoch of training is defined as a single presentation of all input vectors to the filter. The filter is then updated according to the results of all those presentations. Training occurs until a maximum number of epochs occur, the performance goal is met, or any other stopping condition of the training function occurs [Haykin, 2002].

First, third, fifth and seventh order filters considering P_{ave} (in dB) as input and flow as output, optimized with LMS algorithm, were used in this study. For each target flow (low, tidal, medium and high) flow signal of one inspiration/expiration and its corresponding tracheal sound P_{ave} that was assumed to be available for calibration, were used for training and finding the filter coefficients. The filter was trained until the MSE reached a plateau. The obtained filter was then employed to estimate flow from P_{ave} (in dB) for each target flow. Finally, the estimation error was calculated for each flow rate and averaged between the subjects.

3.5.2 Neural Networks

Neural networks are composed of simple elements operating in parallel. These elements are inspired by biological nervous systems. As in nature, the network function is determined largely by the connections between elements. We can train a neural network to perform a particular function by adjusting the values of the connections (weights) between the elements.

Backpropagation Network was created by generalizing the Widrow-Hoff learning rule to multiple-layer networks and nonlinear differentiable transfer functions. Input vectors and the corresponding target vectors are used to train a network until it can

approximate a function. Networks with biases, a sigmoid layer, and a linear output layer are capable of approximating any function with a finite number of discontinuities.

Standard backpropagation is a gradient descent algorithm, in which the network weights are moved along the negative of the gradient of the performance function. The term backpropagation refers to the manner in which the gradient is computed for nonlinear multilayer networks [Freeman & Skapura, 1991].

A feedforward backpropagation Neural Network consists of two layers. The first layer or hidden layer has a *tangent-sigmoid* (tan-sig) activation function, and the second layer or output layer, has a linear activation function *purelin*. Thus, the first layer limits the output to a narrow range, from which the linear layer can produce all values. The output of each layer can be represented by

$$Y_{N\times 1} = f(W_{N\times M} X_{M,1} + b_{N,1}), \tag{3.22}$$

where Y is a vector containing the output from each of the neurons in a given layer, W is a matrix containing the weights for each of the M inputs for all N neurons, X is a vector containing the inputs, b is a vector containing the biases and $f(\cdot)$ is the activation function [Freeman & Skapura, 1991]. The network was created using the neural network toolbox from Matlab 6.1 release 12.1 (The MathWorks).

The network is initialized with random weights and biases, and is then trained using the Levinson-Marquardt algorithm [Freeman & Skapura, 1991]. The weights and biases are updated according to

$$D_{n+1} = D_n - \left[J^T J + \mu I\right]^{-1} J^T e, \tag{3.23}$$

where D_n is a matrix containing the current weights and biases, D_{n+1} is a matrix containing the new weights and biases, e is the network error, J is a Jacobian matrix

containing the first derivative of e with respect to the current weights and biases, I is the identity matrix and μ is a variable that increases or decreases based on the performance function. The gradient of the error surface, g, is equal to $J^T e$.

Calibration Type 1 was employed for the flow estimation method using Neural Networks. Flow signal of four breaths, each from a different target flow, and the features extracted from their corresponding tracheal sound signal (P_{ave}, f_{max}, E_{a5}) were used for training the network. The obtained network was then employed to estimate flow. The first layer of the network, or hidden layer, contained 9 neurons and had a tangent-sigmoid (tansig) activation function. The second layer, or output layer, had a linear activation function, purelin, and one neuron.

3.6 THE EFFECT OF AGE

Considering f_{max} and P_{ave} once the better model describing one of these features and flow was selected, the effect of age on the model parameters was also investigated by dividing the subjects into three age groups: 7.4 ± 2.3 years old (Age group 1), 11.5 ± 1.22 years old (Age group 2) and 30.8 ± 7.25 years old (Age group 3), and estimating the model parameters for each age group. The results were studied to determine whether the model representing flow-sound relationship changes with age.

CHAPTER 4

RESULTS

4.1 PARAMETRIC METHODS

The three models used as parametric models for flow estimation are as follows.

1) Exponential Model: $F_{est} = c_1 \log(P_{ave}) + c_2$, 4.1

2) 2nd degree polynomial Model: $F_{est} = c_1 f_{\max}^{\ 2} + c_2 f_{\max} + c_3$, 4.2

3) Power model: $\log(F_{est}) = c_1 \log(E_{a5}) + c_2$, 4.3

where F_{est} is the estimated flow and c_1, c_2 and c_3 are the model coefficients. The results of these models for estimating flow are presented in the following sections.

4.1.1 Exponential Model Using the Average Power of Tracheal Sound

Tables 4.1 and 4.2 show details of the estimation error for different target flow rates. As it can be observed from the tables, the second type of calibration was superior. However, using either of the calibration approaches, the estimation error was the highest at low flow as expected. The overall estimation error, using the first type of calibration, was 0.19 ± 0.08 for inspiration and 0.24 ± 0.09 for expiration, while the second type of calibration resulted in an overall error of 0.09 ± 0.03 and 0.1 ± 0.04 for inspiration and expiration, respectively. Therefore Type 2 calibration appears to be a better choice.

Table 4.1. Estimation error ($\mu \pm \sigma$) for different target flow rates using P_{ave} and exponential model, during inspiration.

Calibration Type	Low	Tidal	Medium	High
Type 1	0.38 ± 0.06	0.28 ± 0.09	0.15 ± 0.09	0.15 ± 0.06
Type 2	0.14 ± 0.04	0.09 ± 0.05	0.09 ± 0.04	0.1 ± 0.04

Table 4.2. Estimation error ($\mu \pm \sigma$) for different target flow rates using P_{ave} and exponential model, during expiration.

Calibration Type	Low	Tidal	Medium	High
Type 1	0.43 ± 0.07	0.33 ± 0.09	0.21 ± 0.8	0.19 ± 0.09
Type 2	0.23 ± 0.2	0.08 ± 0.04	0.08 ± 0.04	0.09 ± 0.04

4.1.2 2nd Degree Polynomial Model using the Maximum Frequency (f_{max})

Optimizing the Flow Region for Estimation

Table 4.3 displays the MSE of the 2nd degree polynomial model describing flow and f_{max} relationship for different upper X% of flow. The results were not conclusive for a flow region to be superior to others. As a result the upper 40% of the flow was used in the rest of study to be consistent with previous studies.

Table 4.3. MSE ($\mu \pm \sigma$) of the 2nd degree polynomial model describing flow and f_{max} relationship for different upper X% of flow.

X	Inspiration	Expiration
15	0.05 ± 0.04	0.06 ± 0.04
25	0.05 ± 0.02	0.06 ± 0.06
40	0.06 ± 0.02	0.05 ± 0.03
65	0.05 ± 0.02	0.07 ± 0.06
90	0.08 ± 0.07	0.06 ± 0.06

Flow Estimation

Table 4.4 shows the estimation error for different target flow rates when calibration Type I was employed for polynomial model using f_{max}. The overall estimation error in this case was 0.28 ± 0.18 and 0.3 ± 0.18 for inspiration and expiration, respectively. This error was very high and showed that f_{max} could not be considered as a suitable feature for flow estimation. Therefore, no estimation was done using the second type of calibration because it was observed that there was not a strong and consistent relationship between flow and f_{max} when different target flow rates were considered separately.

Table 4.4. Estimation error ($\mu \pm \sigma$) for different target flow rates using f_{max} and 2nd degree polynomial model with calibration Type 1.

	Low	Tidal	Medium	High
Inspiration	0.52 ± 0.22	0.31 ± 0.17	0.28 ± 0.16	0.25 ± 0.17
Expiration	0.61 ± 0.07	0.33 ± 0.09	0.25 ± 0.8	0.27 ± 0.09

4.1.3 Power Model Using Wavelet Transform of Tracheal Sound

Optimizing the Flow Region for Estimation

Tables 4.5 and 4.6 display MSE and correlation coefficient of the power model describing flow and E_{a5} relationship for different upper X% of flow.

The values of MSE and correlation coefficient between actual values of flow and the fitted curves were compared to determine an optimum flow region for deriving the model's coefficients. However, the results were not conclusive for a flow region to be superior to others. Hence, for the sake of consistency with previous studies the upper 40% of flow was used.

Table 4.5. MSE ($\mu \pm \sigma$) of the power model describing flow and E_{a5} relationship for different upper X% of flow.

X	Inspiration	Expiration
15	0.02 ± 0.02	0.03 ± 0.02
25	0.03 ± 0.02	0.03 ± 0.02
40	0.03 ± 0.04	0.04 ± 0.02
65	0.05 ± 0.02	0.04 ± 0.02
90	0.05 ± 0.03	0.06 ± 0.03

Table 4.6. Correlation Coefficient ($\mu \pm \sigma$) of the power model describing flow and E_{a5} relationship for different upper X% of flow.

X	Inspiration	Expiration
15	0.92 ± 0.07	0.91 ± 0.07
25	0.9 ± 0.07	0.9 ± 0.08
40	0.9 ± 0.07	0.91 ± 0.08
65	0.89 ± 0.07	0.9 ± 0.08
90	0.88 ± 0.05	0.89 ± 0.08

Flow Estimation

Tables 4.7 and 4.8 show the estimation error for different target flow rates. The overall estimation error, using the first type of calibration, was 0.14 ± 0.07 for inspiration and 0.21 ± 0.12 for expiration, while second type of calibration resulted in an overall error of 0.19 ± 0.09 and 0.22 ± 0.12 for inspiration and expiration, respectively. In this case, the first type of calibration gave slightly better results, but the error was still high.

Table 4.7. Estimation error ($\mu \pm \sigma$) for different target flow rates using the power model and E_{a5} during inspiration.

Calibration Type	Low	Tidal	Medium	High
Type 1	0.24 ± 0.17	0.1 ± 0.06	0.14 ± 0.13	0.14 ± 0.19
Type 2	0.28 ± 0.19	0.19 ± 0.17	0.17 ± 0.11	0.17 ± 0.11

Table 4.8. Estimation error ($\mu \pm \sigma$) for different target flow rates using the power model and E_{a5} during expiration.

Calibration Type	Low	Tidal	Medium	High
Type 1	0.45 ± 0.32	0.31 ± 0.33	0.16 ± 0.15	0.14 ± 0.08
Type 2	0.59 ± 0.25	0.24 ± 0.21	0.15 ± 0.11	0.17 ± 0.13

4.2 NONPARAMETRIC METHODS

4.2.1 Adaptive Filters

The Estimation errors for different target flow rates using adaptive filters are shown in Tables 4.9 and 4.10 for inspiration and expiration, respectively. Table 4.11 displays the overall error for inspiration and expiration. 3rd order adaptive filter was superior compared to the others in this category; which its results were also comparable with those of the exponential model using P_{ave}.

Table 4.9. Estimation error ($\mu \pm \sigma$) of adaptive filter for different target flow rates during inspiration.

Order of Filter	Low	Tidal	Medium	High
1st order	0.2 ± 0.07	0.13 ± 0.07	0.15 ± 0.1	0.11 ± 0.05
3rd order	0.14 ± 0.07	0.09 ± 0.05	0.1 ± 0.05	0.09 ± 0.05
5th order	0.27 ± 0.11	0.11 ± 0.07	0.1 ± 0.04	0.11 ± 0.06
7th order	0.22 ± 0.11	0.11 ± 0.07	0.1 ± 0.08	0.13 ± 0.07

Table 4.10. Estimation error ($\mu \pm \sigma$) of adaptive filter for different target flow rates during expiration.

Order of Filter	Low	Tidal	Medium	High
1st order	0.23 ± 0.14	0.11 ± 0.05	0.12 ± 0.05	0.11 ± 0.06
3rd order	0.17 ± 0.13	0.1 ± 0.05	0.1 ± 0.04	0.11 ± 0.06
5th order	0.15 ± 0.09	0.1 ± 0.05	0.11 ± 0.06	0.11 ± 0.06
7th order	0.14 ± 0.06	0.1 ± 0.05	0.12 ± 0.08	0.12 ± 0.07

Table 4.11. Overall Estimation Error ($\mu \pm \sigma$) of adaptive filter with different orders.

Order of Filter	Inspiration	Expiration
1st order	0.13 ± 0.05	0.13 ± 0.04
3rd order	0.1 ± 0.03	0.11 ± 0.04
5th order	0.12 ± 0.04	0.11 ± 0.04
7th order	0.12 ± 0.04	0.12 ± 0.04

4.2.2 Neural Networks

There was no stable result when Neural Networks were applied. Estimation error varied from 0.07 to 0.51 for different trials. The results were almost the same for inspiration and expiration. Figures 4.1 displays the output of neural network plant model for one of the subjects.

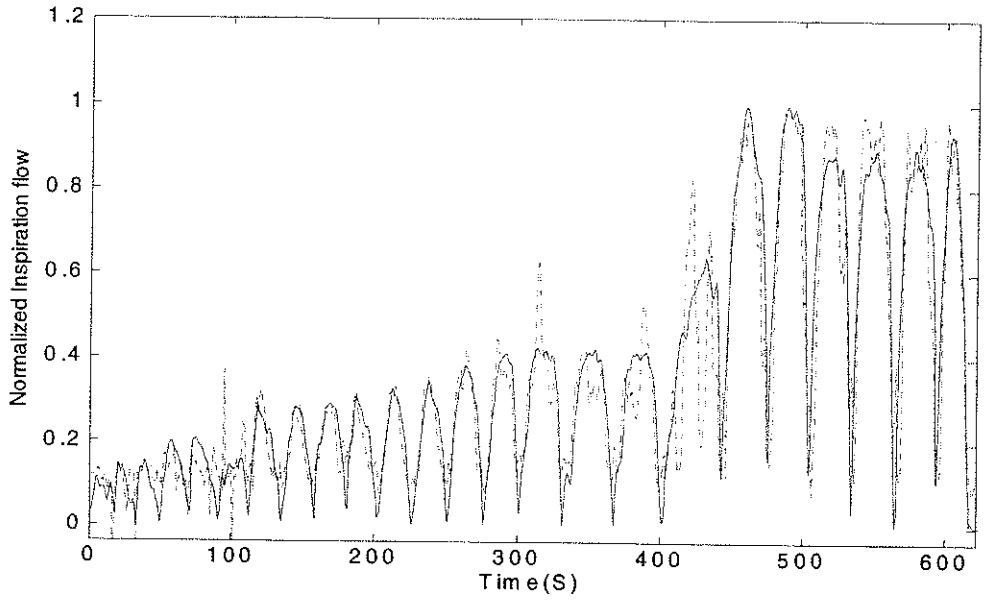

(a)

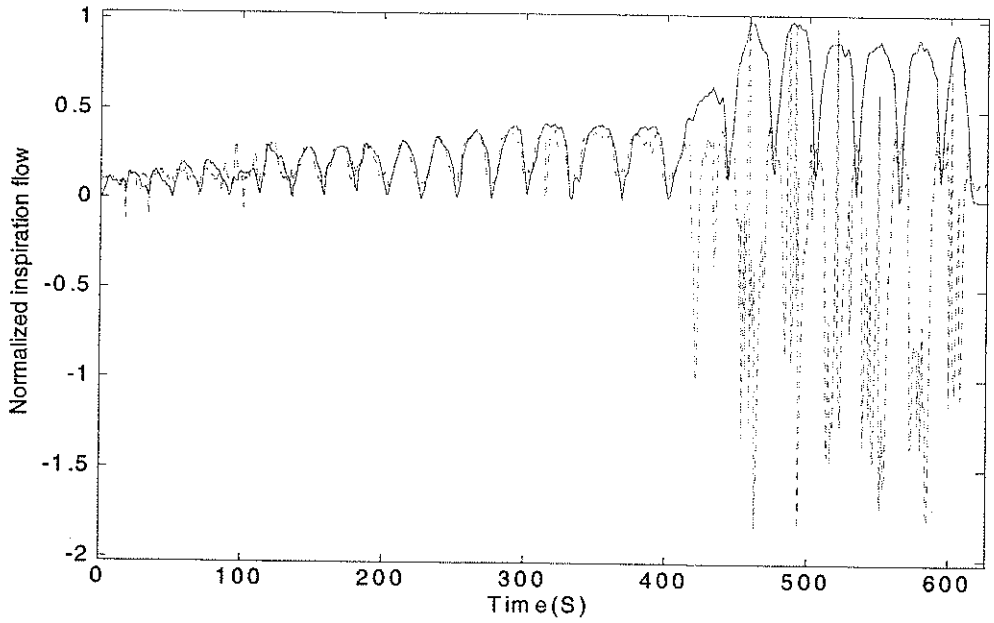

(b)

Figure 4.1. Actual (solid line) and estimated flow (dotted line) for two different trials.

4.3 The Effect of Age

The effect of age on model parameters for $f_{max,}$ and P_{ave} was investigated considering the 2nd degree polynomial for f_{max} and the exponential model for P_{ave}. Coefficients of the 2nd degree polynomial between f_{max} and flow averaged for different age groups are shown in Tables 4.12 and 4.13 for inspiration and expiration, respectively. The results showed a considerable shift of f_{max} toward lower frequencies with age (Figure 4.2). However, there was not a conclusive result for describing the relationship between age and P_{ave}.

Table 4.12. Coefficients of the 2nd degree polynomial relationship between f_{max} and flow during inspiration.

Age group	C_1	C_2	C_3
4-10	0.17 ± 0.73	0.2 ± 0.9	0.02 ± 0.29
10-13	0.69 ± 0.37	-0.19 ± 0.43	0.11 ± 0.13
26-43	2.54 ± 0.51	-1.56 ± 0.51	0.35 ± 0.1

Table 4.13. Coefficients of 2nd degree polynomial relationship between f_{max} and flow during expiration.

Age group	C_1	C_2	C_3
4-10	1.5 ± 1.9	-1.39 ± 2.09	0.45 ± 0.56
10-13	1.9 ± 2.7	-1.85 ± 3.12	0.55 ± 0.87
26-43	2.2 ± 1.4	-1.59 ± 1.04	0.38 ± 0.23

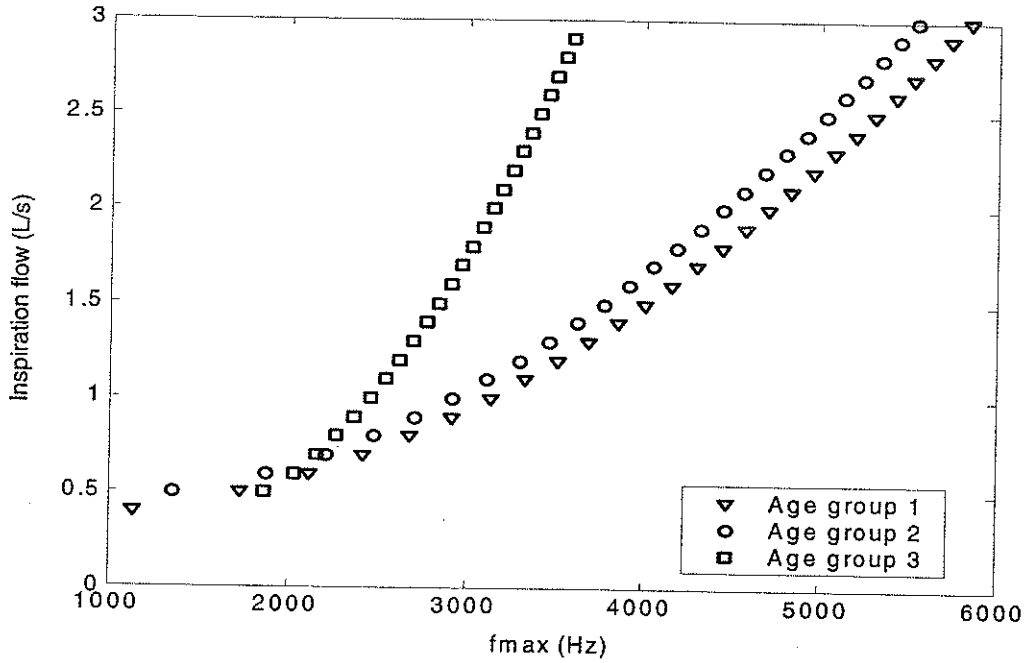

(a)

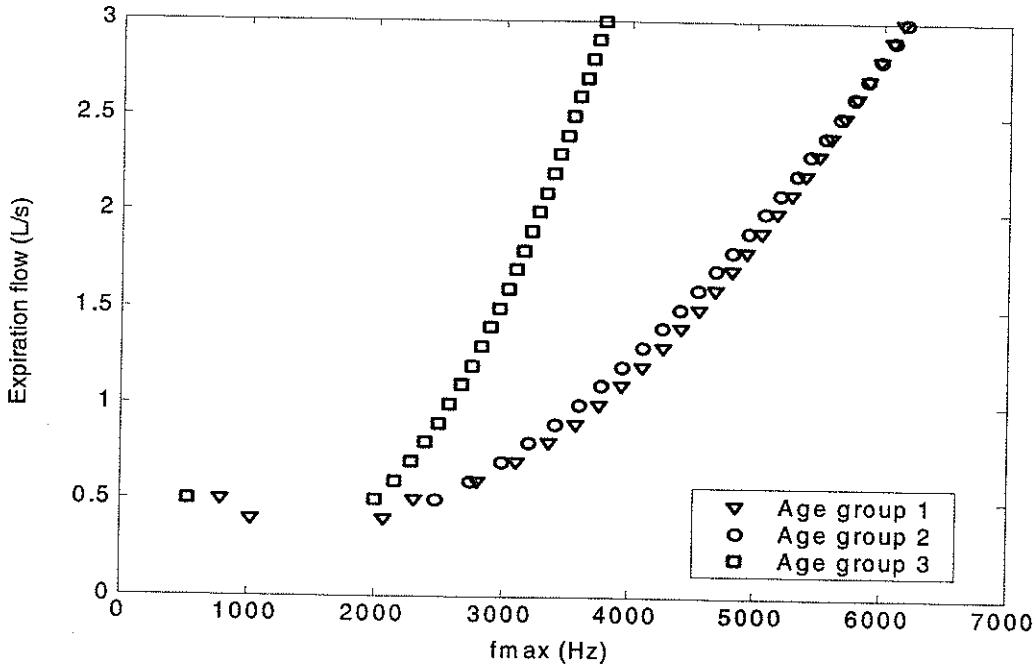

(b)

Figure 4.2. Flow-fmax relationship for each age group for inspiration (a) and expiration (b). The plot shows the average between the subjects in each group.

CHAPTER 5

DISCUSSION & CONCLUSIONS

In this study several features of tracheal sound were investigated for the purpose of estimating flow from tracheal sound. These features included the average power of tracheal sound (P_{ave}), the envelope of the fifth coefficient of the wavelet transform of the signal (E_{a5}) and f_{max}, f_{mean} and f_{peak} of tracheal sound spectrum. The relationship between flow and the features were studied by considering a few models for each feature. Then, the better model representing the relationship between flow and a particular feature (P_{ave}, E_{a5} or f_{max}) was selected for flow estimation. P_{ave} (dB) showed a strong linear relationship with flow with the correlation coefficient about 0.9. The relationship between flow and P_{ave} was best described with an exponential model, which is also in agreement with the results reported in [Yap & Moussavi, 2002]. In this study P_{ave} was calculated over frequency band 150-450 Hz, as this range was reported to be the best frequency range for flow estimation in terms of the estimation error [Yap & Moussavi, 2002].

Among the frequency-based features, only f_{max} had a considerable relationship with flow. This relationship could be described with either a 2nd degree polynomial or an exponential model. The correlation coefficient for the exponential model was about 0.7. A previous research [Lessard & Wong, 1986] showed that a direct linear relationship existed between f_{max} and flow in the range 0.25 L/s to 0.75 L/s but it leveled off as the flow increased beyond 0.75 L/s. However, the results of this study have shown that a 2nd degree polynomial or an exponential model describes the relationship between flow and f_{max} with a much smaller MSE than the linear model. It must be noted that only the mean of upper 15% of the flow and its corresponded tracheal sound was used for modeling in

this study. The aforementioned study did not mention what percentage of target flow was considered. If one approximates the 2nd degree polynomial or exponential model -used in this study- with a piecewise linear model, similar results can be concluded as reported in [Lessard & Wong, 1986]. This implies that the rate of changes of f_{max} with flow becomes smaller at higher flow rates, i.e. above 2 L/s (Figure 4.2).

None of the previous studies had considered the wavelet transform coefficients of the tracheal sound as potential features for flow estimation. In this study, one-dimensional continuous wavelet transform of tracheal sound was calculated using db4 wavelet. The first coefficients of wavelet transform which correspond to lower scales, show rapidly changing details, while the last coefficients display coarse features of the signal. In this study the envelope of the fifth coefficient of the wavelet transform, E_{a5}, was selected for investigating its relationship with flow. The envelope of this coefficient demonstrates the overall trend of the tracheal sound signal while keeping high frequency changes. Among the models we investigated; the best model describing the relationship between flow and E_{a5} was found to be in the form of power relationship model, with a correlation coefficient of 0.92 between $log(E_{a5})$ and $log(flow)$.

After selecting the features of tracheal sound in relation to flow, the models, which had either higher correlation coefficient or less MSE, were chosen for flow estimation. The selected models were exponential model using P_{ave}, 2nd degree polynomial model using f_{max} and power model using E_{a5}.

A major drawback of the flow estimation methods is their dependency on calibration part. Given the vast difference among the subjects, the model for flow estimation for each subject must be calibrated, i.e., the model parameters must be derived

from a few breaths with known flow. Previous reported methods for flow estimation heavily rely on the calibration. The study using tracheal sound envelope [Que et al, 2002] used 50% of the data for calibration and training the model and the other 50% for estimation. In addition, the flow rate was the same in their calibration set and test set. The main problem that is challenging to solve is that when the flow rate changes, the model parameters describing the relationship between tracheal sound feature and flow change too. Hence if the model's parameters are derived from a certain flow rate, it gives a high error when used to estimate a flow rate out of the range of the calibrated flow. This type of error is addressed as underestimation/overestimation error. The other recent study, which used the average power of tracheal sound with an exponential model to estimate flow [Yap & Moussavi, 2002], assumed that a copy of each target flow of the test set to be estimated is available in the calibration set. Therefore, they were able to adjust the model parameters automatically for the three different target flows. They used the same exponential model used in this study. However, they modified the model by a scaling factor. The scaling factor was in the form of a ratio between the average power of the segment that its correspondent flow was being estimated and the average power of the base segments which were used to derive the model parameters:

$$\text{Scaling factor} = \left(\frac{P_{segment}}{P_{base}}\right)^{k}, \qquad 5.1$$

where k is a constant that was determined from the few known breath sounds with flow that they assumed to be available for calibration. For example, if the model parameters, c_1 and c_2, were derived from medium target flow, k consisting of k_{low} and k_{high} was determined by minimizing the error using two known breaths at low and high flow rates, respectively. Therefore, that study assumed that a couple of copies of each target flow

were available at the calibration stage. With this technique, they achieved a low estimation error of less than 6% [Yap & Moussavi, 2002]. However, it should be noted that the low estimation error was due to the existence of the replicas of the every target flow of the test set during the calibration stage.

It has been observed that the model parameters are different for different flow rates. A scaling factor in the form of a ratio between P_{base} and $P_{segment}$ without using the exponent k could be used if a linear relationship between the model parameters and $log(P_{ave})$ or P_{ave} existed. Such possibility was also investigated in this study. However, the change of model parameters as a result of change of target flow was not found to be consistent between the subjects. Therefore, we did not use scaling factor to adjust the model to different flow rates. Instead, two different calibration approaches were used. In both approaches it was assumed that one breath cycle of each of the low, tidal, medium and high target flows can be available for calibration. However, the test set consisted of flow rates out of the range of calibration as well. In approach I of calibration, one set of the model parameters was derived from the four calibration breath cycles, while in approach II of calibration, four sets of model parameters were derived from the one breath cycle at every flow rate and then the data of the test set was divided into four different low, tidal, medium and high flow rates blindly of the flow using E_{a5} and a threshold as described in chapter 3.

The estimation error using calibration approach I was the least (14 ± 7 % and 21 ± 12 % for inspiration and expiration, respectively) when E_{a5} was used for estimation with the power model. However, using calibration approach II, the exponential model employing P_{ave} was superior with an average error of 9 ± 3 % and 10 ± 4 % for inspiration and

expiration, respectively. Although we used the same model as the one used in [Yap and Moussavi, 2002] for P_{ave} and flow, the results of this study indicated higher error. Using a wider range of flow is one reason, as data of Group I included low flow, which would lead to a high error. Dividing the tracheal sound to different target flow regions blind of flow by thresholding the E_{a5} signal, could be another cause of the higher error.

As an alternative to parametric methods for flow estimation, adaptive filters and Neural Networks were also investigated as nonparametric methods. Since there was a linear relationship between flow and $log(P_{ave})$, and it resulted in a lower error of flow estimation in parametric methods of flow estimation, $log(P_{ave})$ was used as the input of the adaptive filters, while the flow of the calibration stage was used as the desired response. For each target flow, a different adaptive filter was used (calibration approach II). Adaptive filters of the first, third, fifth and seventh order were used in this study. The estimation error was least for third order filter which was 10 ± 3 % and 11 ± 4 % for inspiration and expiration, respectively. This shows that there is a correlation between the delayed flow and tracheal sound average power but this correlation decreases with delays greater than one-sixth of the length of inspiration/expiration cycle (about 20 samples).

From the features that were studied in this study, P_{ave}, E_{a5}, f_{max} that showed a considerable relationship with flow, were used as the inputs of Neural Networks. Neural Networks did not give any stable results. Estimation error varied from 7% to 51% for different trials. The reason is probably due to the fact that the training data were about one-fifth of the test data.

It was observed that using all methods, the error was decreasing when target flow increased. There is a threshold flow, which needs to be exceeded so that breath sounds

can be recognized, and at very low flow rates, i.e., lower than 0.3 L/s, the breath sound amplitude does not exceed the background noise (Figure 5.1). This is the reason why all methods lead to very high error for low flow rate.

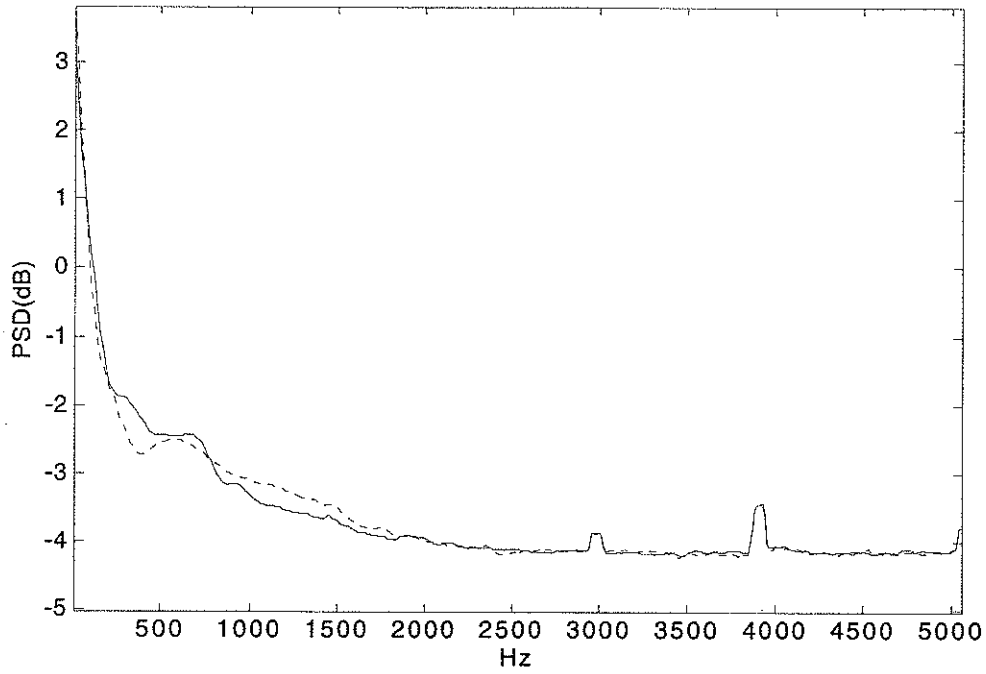

Figure 5.1. Average PSD of low flow (solid line) and background noise (dotted line).

Overall, among different investigated methods and features, the exponential model using P_{ave} with calibration approach II was superior with the least error of 9 ± 3 % and 10 ± 4 % for inspiration and expiration, respectively. Adaptive filtering method using $log(P_{ave})$ was second with an acceptable error of 10 ± 3 % and 11 ± 4 % for inspiration and expiration, respectively. Comparing these with those reported in other studies [Que *et al.*, 2002, Soufflet *et al.*, 1990], the error of the suggested methods in this study was much less although a wider range of flow and a much smaller set of breath for calibration were used.

Our results on aging effect on f_{max} showed that for any target flow, f_{max} is decreasing with age. This result is indirectly in agreement with the findings reported in [Sanchez & Pasterkamp, 1993] that analyzed tracheal sounds in children and adults and found that children with the shorter tracheal lengths had a higher cutoff frequency. They calculated the quartile frequencies below which 25% (Q1), 50% (Q2) and 75% (Q3) of the power in the range of 50 to 2000 Hz was contained, and the spectral edge frequency (SE) below which 95% of the power was found. Above 200 Hz, the cutoff frequency (f_{cut}) was determined after smoothing individual spectrum as the lowest frequency beyond which the power dropped more than 6 dB/200 Hz. They found that children had considerably higher frequencies (Q1, Q2, Q3, SE and f_{cut}) than adults and furthermore, these parameters were inversely correlated with height (r=*-0.88*). There are also similar results reported in [Coleman & Schechter, 1991]. They observed sound spectral characteristics in a physical model of the upper central airways, using varying lengths of a clear plastic pipe and found that natural resonances of longer tubes were lower than those of shorter tubes. As it is discussed in [Sanchez & Pasterkamp, 1993] this is probably an indication that the spectral peak may reflect resonance within the central airway.

The motivation behind this research was to investigate flow-sound relationship thoroughly in order to develop a robust method for flow estimation from tracheal respiratory sound. The thesis contribution in the field of flow estimation was that average power of tracheal sound could be successfully used for estimating flow employing parametric methods and also adaptive filters.

CHAPTER 6

FUTURE WORK

The results of this thesis confirmed that the exponential model using average power of tracheal sound was the better model to estimate flow. Second best model was using adaptive filters while the input was again the average power of the tracheal sound. Therefore, in a sense, these two techniques were similar in their model. These results are encouraging to continue research on flow estimation as an alternative for conventional flow measurement. Since the subjects may occasionally swallow during the respiratory assessment, the current techniques must be used with a swallowing detection algorithm so that the swallow segments are detected and removed.

In addition, there is room for improvement in the signal acquisition part. Lower errors would be obtained using a higher quality tracheal sound with low noises and artifacts.

One of the disadvantages of this study is that data from four different target flows were used in calibration. In practical situations it may not be possible to have diverse target flows during calibration especially when studying young children or patients with neurological impairment. However as the relationship between flow and tracheal sound features -used in this study- changes with target flow, further investigation is needed to find a more robust method of flow estimation.

From the statistical point of view, when average power of tracheal sound is calculated, only changes in variance of tracheal sound signal is being considered. Further studies may consider features, which incorporate higher order statistical properties of the signal.

REFERENCES

M. Abella, J. Formolo and D. G. Penny, "Comparison of the Acoustic Properties of six popular Stethoscopes", *J. Acoust. Soc. Am.*, vol. 91, pp. 2224-2228, 1992.

A. Avital, E. Bar-Yishay, C. Springer and S. Godfrey, "Bronchial Provocation Tests in Young Children Using Tracheal Auscultation", *J.Pediatrics*, vol. 112, pp. 591-594, 1988.

R. C. Beckerman, M. J. Wegmann and W. W. Waring, "Tracheal Breath Sounds for Detection of Apnea in Infants and Children", *Crit. Care Med*, vol. 10, pp. 363-366, 1982.

A. B. Bohadana, N. Massin, D. Teculescu and R. Peslin, "Tracheal Wheezes During Methacholine Airway Challenge (MAC) in Workers Exposed to Occupational Hazards", *Respir. Med.*, vol. 88, pp. 581-587, 1994.

T. Brancatisano, P. W. Collett and L. A. Engel, "Respiratory Movements of the Vocal cords", *J. Appl. Physiol.*, vol. 54, pp. 1269-1276, 1983.

O. Bratteli and P. Jorgenson, "Wavelts Through a Looking Glass: The World of the Spectrum", Boston, MA: Birkhäuser, 2002.

G. Charbonneau, M. Sudraud and G. Soufflet, "A Method to Evaluate Flow Rate from Breath Sounds", *Bull. Eur. Physiopathol. Respir.*, vol. 23, pp. 265-270, 1987.

G. Chi-Lem, Y. Inaba, M. Greenberg, H. Pasterkamp, "Critical Flow to Generate Breath Sound Does not Change During Bronchial Constriction", *Am. J. Respir. & Crit. Care Med.*, vol. 157(3), pp. A540, 1997.

R. F. Coleman, G. L. Schechter, "A Basic Model to Study Acoustic Evaluation of Airway Obstruction", *Arch Otoralyngol Head Neck Surg.*, vol. 117, pp.1144-1149, 1991.

J. E. Earis and B. M. G. Cheetham, "Future Perspective of Respiratory Sound Research", *Eur. Respir. Rev.*, vol. 10(77), pp. 641-646, 2000.

K. A. East and T.D. East, "Computerized Acoustic Detection of Obstructive Apnea", *Comput. Methods Programs Biomed.*, vol. 21, pp. 213-220, 1985.

J. A. Freeman and D. M. Skapura, Neural networks: Algorithms, Applications and Programming Techniques. Addison Wesley Longman, 1991, pp. 89-105.

P. Forgacs, "The Functional Basis of Pulmonary Sounds", *Chest*, vol. 73, pp. 399-405, 1978.

J. J. Fredberg, "A Model Prospective of Lung Response", *J. Acoust. Soc. Am.* vol. 60, pp. 962-966.

N. Gavriely and D. W. Cugell, "Airflow Effect on Amplitude and Spectral Content of Normal Breath Sounds", *J. Appl. Physiol.*, vol. 80, pp. 5-13, 1996.

N. Gavriely, Y. Plati and G. Alroy, "Spectral Characteristics of Normal Breath Sounds", *J. Appl. Physiol.* vol. 50, pp. 307-314, 1981.

V. P. Harper, H. Pasterkamp and G. R. Wodicka, "An Acoustic Model of the Respiratory Tract", *IEEE Transactions on Biomedical Engineering.* vol. 48(5), pp. 543-550, 2001.

V. P. Harper, H. Pasterkamp, H. Kiyokawa and G. R. Wodicka, "Modeling and Measurement of Flow Effects on Tracheal Sounds", *IEEE Transactions on Biomedical Engineering.* vol. 50(1), pp. 1-10, 2003.

S. Haykin, Adaptive Filter Theory. Upper Saddle River, NJ: Prentice-Hall, 2002.

W. Hida, H. Miki, Y. Kikuchi, C. Miura, N. Iwase, Y. Shimizu and T. Takishima, "Home Sleep Monitor for Detecting Apnea Episodes by Nasal Flow and Tracheal Sound Recordings", *Tohoku J. Exp. Med.*, vol. 156, pp. 137-142, 1988.

H. Hudde and H. Slatky, "The Acoustical Input Impedance of Excised Human Lungs: Measurement and Model Matching", *J. Acoust. Soc. Am.*, vol 86, pp. 475-492, 1989.

K. Ishizaka, M. Matsudaira and T. Kaneko, "Input Acoustic Impedance Measurement of Subglottal System", *J. Acoust. Soc. Am.* vol. 60, pp. 190-197, 1976.

A. C. Jackson, C. A. Giudanella and H. L. Dorkin, "Density Dependance of Respiratory System Impedance between 5 and 320 Hz in Humans", *J. Appl. Physiol.*, vol. 67, pp. 2323-2330, 1989.

Y J. Jeon, Y. J. Yi, J. J. Im, N. G. Kim, "Classification of Normal Person and Pulmonary Function Disease Patients based on the Respiratory Sound from Trachea", *Proceeding of the First Joint BMES/EMBS Conference*, pp 334-335, 1999.

S. S. Kraman, H. Pasterkamp, M. Kompis, M. Takase and G. R. Wodicka, "Effect of Breathing Pathways on Tracheal Sound Spectral Features", *Respir. Physiol.*, vol. 111, pp. 295-300, 1998.

P. E. Krumpe and J. M. Cummiskey, "Use of Laryngeal Sound Recordings to Monitor Apnea" , *Am. Rev. Respir. Dis.*, vol. 122, pp. 797-801, 1980.

P. Leblank, P. T. Machlem and W. R. D. Ross. "Breath Sounds and Distribution of Pulmonary Ventilation", *Am. Rev. Respir. Dis.*, vol. 102, pp. 10-16, 1970.

C .S. Lessard and W. C. Wong, " Correlation of Constant Flow Rate with frequency Spectrum of Respiratory Sounds When Measure at the Trachea", *Trans. On Biomed. Eng.*, vol. 33(4), pp. 461-463 , 1986.

C. S. Lessard, W. C. Wong and J.J. Im, "Synopsys of Tracheal Sounds", *Proc. IEEE Eng. in Med. and Biol. Soc.*, vol. 3, pp. 1076-1077, 1988.

S. G. Mallat, "A Theory of Multi-Resolution Signal Decomposition: The Wavelet Representation", *IEEE Trans. Pattern Anal. Machine Intel.* vol. 11(5), pp. 578-586, 1989.

Z. Moussavi, M. T. Leopando, H. Pasterkamp and G. Rempel, "Computerized Acoustical Respiratory Phase Detection without Airflow Measurement", *Med. and Biol. Eng. and Comput.*, vol. 38(2), 198-203, 2000.

M. J. Mussel and Y. Miyamoto, "Comparison of Normal Respiratory Sounds Recorded from the Chest and Trachea at Various Respiratory Airflow Levels", *Front. Med. Biol. Eng.*, vol. 4(2), pp. 73-85, 1992.

M. J. Mussel, Y. Nakazano, Y. Miyamoto, S. Okabe and T. Takishima, "Distinguishing Normal and Abnormal Tracheal Breathing Sounds by Principal Component Analysis", *Jpn. J. Physiol.*, vol 40, pp. 713-721, 1990.

L. I. Nemerovskii, "Analysis of a Pulmophonogram for Assessing Local Pulmonary Ventilation", *Med. Tekh.*, pp 39-4, 1980.

D. E. Olson, M. Bogyi, D. B. Schwartz and J. R. Hammersley, "Relationship of Tracheal Soundsto Airflow", *Am. Rev. Respir. Dis.*, vol. 129, pp. 256, 1984.

D. E. Olson and J. R. Hammersley, "Mechanism of Lung Sound Generation", *Semin. Respir. Med.*, vol. 6, pp. 171-179, 1985.

A. V. Oppenheim and R.W. Schafer, Discrete-Time Signal Processing, 2nd ed., Prentice-Hall, 1998.

H. Pasterkamp, S. S. Kraman and G. R. Wodicka, "Respiratory Sounds. Advances beyond the Stethescope", *Am. J. Respir., Crit. Care Med.*, vol. 156, pp. 974-987, 1997.

H. Pasterkamp, J. Schafer and G. R. Wodicka, "Posture Dependent Change of Tracheal Sounds at Standardized Flows in Patients with Obstructive Sleep Apnea", *Chest*, vol. 110, pp. 1493-1498, 1996.

Y. Ploysongsang, J. A. P. Pare, P. T. Macklem, "Correlation of Regional Breath Sound with Regional Ventilation in Emphysema", *Am. Rev. Respir. Dis.*, vol. 126, pp. 526-529, 1982.

C. L. Que, C. Kolmaga, L. G. Durand, S. M. Kelly and P. T. Macklem, "Phonospirometry for Noninvasive Measurement of Ventilation: Methodology and Preliminary Results", *J. Appl. Physiol.*, vol. 93, pp. 1515–1526, 2002.

S. Rietveld and L. H. Rijssenbeek-Nouwens, "Diagnostics of Spontaneous Cough in Childhood Asthma: Results of Continuous Tracheal Sound Recording in the Homes of Children", *Chest,* vol. 110, pp. 1493-1498, 1996.

L. Sanchez and H. Pasterkamp, "Tracheal sound spectra depend on body height", *Am. Rev. Respir. Dis.* vol. 148, pp. 1083-1087, 1993.

A. Sanna, P. Lorimier, B. Dachy, A. D'Hondt and R. Sergysels, "Value of Monitoringof Tracheal Respiratory Sounds in the Diagnosis of Nocturnal Respiratory Dysrhythmias", Acta. Clin. Belg., vol. 46, pp. 159-164, 1991.

B. E. Shykoff, Y. Ploysongsang and H. K Chang, "Airflow and Normal Lung Sounds", *Am. Rev. Respir. Dis.*, vol. 137, pp. 872-876, 1988.

G. Soufflet, G. Charbonneau, M. Polit, P. Attal, A. Denjean, P. Escourrou and C. Gaultier, "Interaction Between Tracheal Sound and Flow rate: A Comparison of Some Different Flow Evaluation from Lung Sounds", *IEEE Trans. On Biomed. Eng.*, vol. 37(4), pp. 384-391, 1990.

S. C. Tarrant, R. E. Ellis, F. C. Flack and W. G. Selley, "Comparative Review of Techniques for Recording Respiratory Event at Rest and during Deglutition", *Dysphagia,* vol. 12, pp. 24-38, 1997.

Wavelet Toolbox (2.1) User's Guide, The MathWorks.

J. W. Van Den Berg, "An Electrical Analogue of the Trachea, Lungs and Tissues", *Acta Physiol. Pharmacol. Neerlandica.*, vol. 9, pp. 361-385, 1960.

G. R. Wodicka, K.N. Stevens, H.L. Golub, E.G. Cravalho and D.C. Shannon, "A Model of Acoustic Transmission in the Respiratory System", *IEEE Trans. Biomed. Eng.*, vol 36, pp. 925-934, 1989.

F. T. Wooten, W. W. Waring, M. J. Wegmann, W. F. Anderson and J. D. Conley, "Method of Respiratory Sound Analysis", *Med. Instrum.*, vol. 12, pp. 254-257, 1978.

Y. L. Yap and Z Moussavi, "Acoustical Airflow Estimation From Tracheal Sound Power," *Proc. IEEE CCECE* , vol. 2, pp. 1073-1076, 2002.

M. Yonemaru, K. Kikuchi, M. Mori, A. Kawai, T. Abe, T. Kawashiro, T. Ishihara and T. Yokoyama, "Detection of Tracheal Stenosis by Frequncy Analysis of Tracheal Sounds", *J. Appl. Physiol.*, vol. 75, pp. 605-612, 1993.